





## 22 **Abstract**

23 Water quality problems in the Chesapeake Bay Watershed (CBW) are expected to exacerbate  
24 under climate variability and change. However, climate impacts on agricultural lands and  
25 resultant nutrient loads into surface water resources are largely unknown. This study evaluates  
26 the impacts of climate variability and change on two adjacent watersheds in the Coastal Plain of  
27 the CBW, using Soil and Water Assessment Tool (SWAT) model. We prepared six climate  
28 sensitive scenarios to assess the individual effects of variations in CO<sub>2</sub> concentration (590 and  
29 850 ppm), precipitation increase (11 and 21 %) and temperature increase (2.9 and 5.0 °C), and  
30 considered the predicted climate change scenario using five general circulation models (GCMs)  
31 under the Special Report on Emissions Scenarios (SRES) A2 scenario. Using SWAT model  
32 simulations from 2001 to 2014, as a baseline scenario, the predicted water and nitrate budgets  
33 under climate variability and change scenarios were analyzed at multiple temporal scales.  
34 Compared to the baseline scenario, precipitation increase of 21% and elevated CO<sub>2</sub> concentration  
35 of 850 ppm significantly increased stream flow and nitrate loads by 50 % and 52 %, respectively,  
36 while, temperature increase of 5.0 °C reduced stream flow and nitrate loads by 12 % and 13 %,  
37 respectively. Under the climate change scenario, annual stream flow and nitrate loads showed an  
38 average increase of nearly 40 %, relative to the baseline scenario. Differences in hydrological  
39 responses observed from the two watersheds were primarily attributed to contrasting land use  
40 and soil characteristics. The watershed with larger percent croplands indicated increased nitrate  
41 yield of 0.52 kg N·ha<sup>-1</sup> compared to the one with less percent croplands under the climate change  
42 scenario, due to increased export of nitrate derived from fertilizer. The watershed dominated by  
43 poorly-drained soils showed a lower increase in nitrate yield than one dominated by well-drained  
44 soils, due to a high potential of nitrate loss in surface runoff and enhanced denitrification. To



45 mitigate increased nitrate loads potentially caused by climate change, the enhanced  
46 implementation of conservation practices would be necessary for this region in the future. These  
47 findings assist watershed managers and regulators as they seek to establish effective adaptation  
48 strategies to mitigate water quality degradation in this region.

49

50

51

52

53

54

55

56

57

58

59

60

61

62



## 63 1 Introduction

64 The Chesapeake Bay (CB) is the largest and most productive estuary in the Mid-Atlantic  
65 region of the United States (US). The Chesapeake Bay Watershed (CBW) covers an area of  
66 166,000 km<sup>2</sup> and is home to more than 18 million people and 3,600 species of plants and animals  
67 (Chesapeake Bay Program, 2016). Despite significant restoration efforts, the health of the Bay  
68 has continued to deteriorate, primarily due to excessive nutrients and sediment loadings from  
69 agricultural lands (Rogers and McCarty, 2000). Najjar et al. (2010) suggested that the current  
70 water quality problems in the Bay are expected to worsen under climate variability and change.  
71 General Circulation Models (GCMs) have projected increases in temperature and precipitation of  
72 up to 5.0 °C and 21 %, respectively, by the end of this century in the CB region (Najjar et al.,  
73 2009), which could lead to substantial changes in the hydrology and nitrogen (N) cycle. For  
74 instance, Howarth et al. (2006) reported that greater precipitation is anticipated to increase N  
75 loads to the CB by ~ 65%. With precipitation and temperature changes, elevated CO<sub>2</sub>  
76 concentration affecting stomatal conductance has also been viewed as one of decisive factors  
77 modifying watershed hydrological processes (Chaplot, 2007; Wu et al., 2012a and 2012b).

78 Numerous studies have been conducted to demonstrate the impacts of changes in CO<sub>2</sub>  
79 concentration, precipitation and temperature on stream flow and N loads. Elevated CO<sub>2</sub>  
80 concentration is predicted to increase stream flow by reduction of evapotranspiration (ET) that  
81 results from a decrease in plant stomatal conductance (Field et al., 1995; Jha et al., 2006; Wu et  
82 al., 2012a and 2012b). Jha et al. (2006), for example, showed that a doubling of CO<sub>2</sub>  
83 concentration increased water loads by ~ 36 % in the upper Mississippi river basin. Precipitation  
84 increase/decrease was found to directly cause the rise/fall of stream flow levels (Jha et al., 2006;  
85 Ficklin et al. 2009; Wu et al., 2012a; Praskievicz, 2014; Uniyal et al., 2015). Similarly, the study



86 by Ficklin et al. (2009) found that precipitation change of + 20 and – 20 % led to changes in  
87 water loads by nearly + 17 and – 14 %, respectively, in the San Joaquin River watershed,  
88 California. Temperature increase was reported to reduce stream flow during summer seasons  
89 due to the intensified ET values, but increase stream flow during winter seasons due to an  
90 upsurge of snow melting (Jha et al., 2006; Ficklin et al. 2009; Wu et al., 2012a; Ficklin et al.,  
91 2013; Praskievicz, 2014). Interestingly, in most studies, the responses of N loads to climate  
92 variability were found to be similar to stream flow (Ficklin et al. 2009; Wu et al., 2012a;  
93 Praskievicz, 2014; Gombault et al., 2015). According to the projected climatic conditions (e.g.,  
94 elevated CO<sub>2</sub> concentration, precipitation and temperature increases) illustrated in Najjar et al.  
95 (2009), substantial variations in stream flow and N loads are anticipated in the CBW. Therefore,  
96 it is important to investigate potential climate change impacts on watershed hydrological  
97 processes to efficiently mitigate water quality degradation.

98         However, climate change impacts on hydrological processes have not been fully  
99 investigated in the CB region. Howarth et al. (2006) attempted to quantify N loads under  
100 modified climate conditions, but their projections relied on the statistical relationships between  
101 river discharge/precipitation and N loads. Lee et al. (2015) predicted changes in stream flow and  
102 nitrate loads at the outlet of the watershed in response to climate variability (e.g., elevated CO<sub>2</sub>  
103 concentration, precipitation and temperature increase). However, their results did not  
104 demonstrate climate change impacts on hydrology and nutrient cycles within a watershed system  
105 (Lee et al., 2015). To cope with climate change-driven modifications, it is imperative to have an  
106 understanding of a wide range of changes in hydrological processes (Najjar et al., 2010). A  
107 simple projection of the future trend of sediment and nutrient loadings would not be sufficient to  
108 prepare strategies to curb climate change impacts. N reduction using conservation practices is



109 most effective when based on comprehensive insight into watershed hydrologic processes  
110 (McCarty et al., 2014). Moreover, responses of watershed hydrological processes to climate  
111 variability and change can vary by watershed characteristics (e.g., land use and soil drainage  
112 conditions). For example, cropland area was found to be positively correlated with in-stream  
113 nitrate concentration in this region (Jordan et al., 1997; Hively et al., 2011; McCarty et al., 2014;  
114 Lee et al., 2016). Furthermore, field studies showed that watersheds with a greater area of  
115 cropland released a higher amount of nitrate than areas with less cropland, mainly due to  
116 agricultural N inputs (Jordan et al., 1997; Hively et al., 2011; McCarty et al., 2014). Thus,  
117 climate change can lead to greater nitrate export from watersheds with a larger percent cropland  
118 area, due to increased export of N from fertilizer application. Additionally, different soil  
119 characteristics also can lead to different responses in watershed-scale water and N cycles under  
120 climate change. The study by Chiang (1971) showed that well-drained soils with a high  
121 infiltration rate promote water percolation, increasing groundwater contribution to stream flow.  
122 Nitrate leaching was also found to frequently occur in well-drained soils (Lee et al., 2016). In  
123 contrast, poorly-drained soils with a low infiltration rate provide anaerobic conditions conducive  
124 to denitrification, resulting in nitrate removal in soils and groundwater (Denver et al., 2010; Lee  
125 et al., 2016; Sharifi et al., 2016). For example, prior converted croplands, which are also known  
126 as “currently farmed historical wetlands”, often associated with areas of poorly-drained soil were  
127 also shown to have prominent impacts on reducing agrochemical loadings in this region during  
128 winter seasons, when ET is low which results in a higher groundwater table (Tiner and Burke,  
129 1995; Denver et al., 2014; McCarty et al., 2014; Sharifi et al., 2016). Artificial drainage systems  
130 in agricultural lands are also widely developed on poorly-drained soils in this region, resulting in  
131 an increase of water and nutrient transport from lands to nearby streams through surface runoff



132 (McCarty et al., 2008; Fisher et al., 2010). Therefore, water and nitrate fluxes in the watersheds  
133 with different soil characteristic would show different responses to climate variability and  
134 change.

135 Nitrate export from Coastal Plain watersheds was found to be substantially greater than  
136 export from other regions of the CBW, due to the relatively high abundance of croplands (Ator  
137 and Denver, 2012). Recent observations from two adjacent watersheds with contrasting land use  
138 (cropland-dominant vs. forest-dominant) and soil characteristics (well-drained vs. poorly-drained)  
139 on the Coastal Plain were shown to have distinctive characteristics of fate and transport, both for  
140 streamflow and nitrate loads (McCarty et al., 2008; Lee et al., 2016; Sharifi et al., 2016).

141 This study aimed at evaluating the impacts of potential climate variability and change on  
142 water and nitrate budgets in the two adjacent watersheds on the Coastal Plain of the CBW, using  
143 the Soil and Water Assessment Tool (SWAT) model. This process-based water quality model  
144 has been widely used to predict climate change impacts on numerous watersheds (Gassman et al.,  
145 2007; Luo et al., 2013; Uniyal et al., 2015). We prepared six climate sensitivity scenarios to  
146 assess the individual effects of changes in CO<sub>2</sub> concentration (590 and 850 ppm), precipitation  
147 (11 and 21 %) and temperature (2.9 and 5.0 °C), and the GCM-based climate change scenario to  
148 evaluate the long-term watershed hydrological processes under projected future climate  
149 conditions. We first analyzed climate change impacts on water and nitrate budgets considering  
150 modified hydrology, N cycle, and crop growth. Then, comparative analyses between two  
151 watersheds were conducted to identify critical landscape characteristics that profoundly affect  
152 nitrate loads under climate variability and change, and finally suggestions were provided for  
153 conservation practices to improve the resilience of coastal watersheds to the future climate  
154 change in this region.



155 **2 Materials and Methods**

156 **2.1 Study area**

157 This study was undertaken on two adjacent watersheds, Tuckahoe Creek Watershed  
158 (TCW, ~220.7 km<sup>2</sup>) and Greensboro Watershed (GW, ~290.1 km<sup>2</sup>). They are sub-watersheds of  
159 the Choptank River Watershed located in the Coastal Plain of the CBW (Figure 1). The  
160 Choptank River Watershed is one of the Conservation Effects Assessment Project (CEAP)  
161 Benchmark watersheds of the United States Department of Agriculture (USDA), Agricultural  
162 Research Services (ARS). The US Environmental Protection Agency (USEPA) has listed this  
163 watershed, as “impaired” under Section 303(d) of the 1972 Clean Water Act, primarily due to the  
164 excessive nutrients and sediment loadings (McCarty et al. 2008). The two adjacent sub-  
165 watersheds have distinctive characteristics considering the distribution of land use and soil  
166 drainage conditions (Figure 2 and Table 1). The TCW is dominated by agricultural lands (54 %)  
167 and forest (32.8 %) with well-drained soils, classified as hydrologic soil groups (HSG) – either A  
168 or B. These soils account for 56% of the total watershed and 69.5 % of the agricultural lands  
169 (Figure 2). Thus, water and nitrate fluxes tend to be easily percolated/leached into soils and  
170 groundwater, and thus groundwater flow is considered as a major water pathway for nutrient  
171 fluxes to streams in TCW (Lee et al., 2016). In comparison, forest (48.3 %) is the major land use  
172 type in GW, followed by agricultural (36.1 %). Soils that are poorly-drained ((HSG) – C or D)  
173 occupy 75 % of the total area and 67.2 % of agricultural lands, which results in a low infiltration  
174 and high denitrification.

175 [Insert Figure 1. The location of Tuckahoe Creek Watershed (left) and Greensboro Watershed  
176 (right)]



177 [Insert Figure 2. The physical characteristics of Tuckahoe Creek Watershed (left) and  
178 Greensboro Watershed (right); (a) land use, (b) hydrologic soil groups, and (c) elevation]

179 [Insert Table 1. Soil properties and land use distribution of Tuckahoe Creek Watershed (TCW)  
180 and Greensboro Watershed (GW)]

181

## 182 **2.2 Soil and Water Assessment Tool (SWAT)**

183 SWAT is a process-based watershed model, developed to assess the impact of human  
184 activities and land use on water and nutrient cycles within agricultural watersheds (Netisch et al.,  
185 2011). SWAT divides a watershed into sub-watersheds using a Digital Elevation Model (DEM),  
186 and each sub-watershed is further divided into hydrological response units (HRUs) based on a  
187 unique combination of land use, soil type, and slope. Model simulation is performed at the HRU  
188 level, and the simulated outputs aggregated at the sub-watershed and then further at the  
189 watershed level through routing processes. The amount of surface runoff and infiltration are  
190 calculated based on Soil Conservation Service (SCS) Curve Number (CN) method, and the CN  
191 values are updated daily based on soil permeability, land use type, and antecedent soil water  
192 conditions. Water infiltrated into soils is either delivered to streams through lateral flow or to  
193 groundwater. The groundwater portion is then either transported to streams, or percolated into  
194 the deep groundwater aquifer. Both inorganic and organic forms of N are simulated with the  
195 SWAT model. The amount of nitrate in soils increases by nitrification, mineralization, and  
196 fertilization, but decreases through denitrification and plant uptake. Nitrate fluxes can move via  
197 surface runoff, lateral flow, groundwater flow, and leaching.



198 SWAT also has the capability of simulating the impacts of CO<sub>2</sub> concentration on ET,  
199 plant stomatal conductance, and biomass accumulations. We used the Penman-Monteith method  
200 to consider CO<sub>2</sub> effects on ET. It calculates potential ET regarding plant canopy resistance that  
201 is adjusted by CO<sub>2</sub> concentration as shown in Eq. (1).

$$202 \quad r_c = r_l \times [(0.5 \cdot LAI) \cdot (1.4 - 0.4 \times (CO_2 / 330))]^{-1} \quad (1)$$

203 where  $r_c$  is plant canopy resistance,  $r_l$  is the minimum effective stomatal resistance of a single  
204 leaf, and  $LAI$  is the leaf area index of the canopy. According to Eq. (1) elevated CO<sub>2</sub>  
205 concentration decreases plant canopy resistance, subsequently reducing ET regarding the  
206 relationship with plant canopy resistance. Refer to Neitsch et al. (2011) for details on the  
207 Penman-Monteith method. The impacts of CO<sub>2</sub> concentration on plant stomatal conductance is  
208 simulated using a function of CO<sub>2</sub> as shown in Eq. (2). The equation simulates the linear  
209 reduction of conductance with increasing CO<sub>2</sub> and estimates 40 % reduction in leaf conductance  
210 for all plants when CO<sub>2</sub> concentration is doubled (Neitsch et al., 2012).

$$211 \quad g_{l,co_2} = g_l \times [1.4 - 0.4 \times (CO_2 / 330)]^{-1} \quad (2)$$

212 where  $g_{l,co_2}$  is the leaf conductance modified to reflect CO<sub>2</sub> effects, and  $g_l$  is the leaf  
213 conductance without the effect of CO<sub>2</sub>.

214 The simulation of the crop growth in SWAT is based on potential heat unit theory.  
215 SWAT considers the impacts of CO<sub>2</sub> concentration on crop biomass growth by modifying  
216 radiation-use efficiency (RUE) of the plant as follows:

$$217 \quad RUE = \frac{100 \cdot CO_2}{CO_2 + \exp(r_1 - r_2 \cdot CO_2)} \quad (3)$$



218 where  $RUE$  is radiation-use efficiency of a plant, and  $r_1$  and  $r_2$  are coefficients.

$$219 \quad \Delta bio = RUE \cdot H_{phosyn} \quad (4)$$

220 where  $\Delta bio$  is a potential increase in plant biomass on a given day and  $H_{phosyn}$  is the amount of  
221 intercepted photosynthetically active radiation on a given day.

222

### 223 **2.3 Baseline SWAT input data**

224 Climate and geospatial data needed for SWAT simulation are summarized in Table 2.

225 Daily precipitation and temperature were obtained from three meteorological stations operated  
226 by the National Oceanic and Atmospheric Administration (NOAA) National Climate Data  
227 Center (NCDC) at Chestertown, Royal Oak, and Greensboro (USC00181750, USC00187806,  
228 and US1MDCL0009, respectively). Due to data unavailability, humidity, wind speed, and solar  
229 radiation were generated using the SWAT built-in weather generator (Neitsch et al., 2011).

230 Monthly stream flow data were downloaded from US Geological Survey (USGS) gauge stations  
231 on the Tuckahoe Creek near Ruthsburg (USGS#01491500) and the Choptank River near  
232 Greensboro (USGS#01491000) (Figure. 1). The USGS LOAD ESTimator (LOADEST, Runkel  
233 et al. (2004)) was used to generate continuous monthly nitrate loads from nitrate grab sample  
234 data that were obtained from the Chesapeake Bay Program (CBP, TUK#0181) for TCW and  
235 USGS gauge station (USGS#01491000) for GW. The land use and soil maps, and DEM were  
236 prepared as shown in Table 2.

237 [Insert Table 2. List of SWAT model input data]



238 We identified representative agricultural practices for this region using multiple  
239 geospatial data (Lee et al., 2016). Major crop rotations and their year to year placement was  
240 derived through analysis of the USDA-National Agricultural Statistics Service (NASS) Cropland  
241 Data Layer (CDL) for the period of 2008 – 2012. We assumed that crop rotation and land use  
242 did not change over the simulation period so that agricultural N input did not vary for the  
243 baseline and climate change scenarios. Detailed agricultural management information (e.g., the  
244 amount, type, and application timing of fertilizer, and planting and harvesting timings of  
245 individual crops) was developed through literature review and communications with local  
246 experts (Table A1). Detailed information about the development of crop rotation and land  
247 management is available in Lee et al. (2016).

248

#### 249 **2.4 Baseline SWAT calibration and validation**

250 SWAT model runs were performed at a monthly time step for 16 years; these include a 2-  
251 year warm-up (1999 – 2000), 8-year calibration (2001 – 2008), and 6-year validation period  
252 (2009 – 2014). Critical parameters used for model calibration were selected based on previous  
253 studies conducted in this region (Sexton et al., 2010; Yeo et al., 2014; Lee et al., 2016) and  
254 allowable ranges of these parameters were derived from literature presented in the caption of  
255 Table 3. Stream flow parameters were first manually calibrated and then nitrate parameters were  
256 adjusted following the model calibration guideline (Arnold et al., 2012). A set of parameters,  
257 that produced the best model performances and fulfilled model performance criteria suggested by  
258 Moriasi et al. (2007), were chosen for model validation. Model performance was evaluated  
259 using the following statistics: Nash-Sutcliffe Efficiency coefficient (*NSE*), Root Mean Square  
260 Error (*RMSE*)-Standard deviation Ratio (*RSR*), and Percent bias (*P – bias*).



$$261 \quad NSE = 1 - \left[ \frac{\sum_{i=1}^n (O_i - S_i)^2}{\sum_{i=1}^n (O_i - \bar{O})^2} \right] \quad (5)$$

$$262 \quad RSR = \frac{RMSE}{STDEV_{obs}} = \left[ \frac{\sqrt{\sum_{i=1}^n (O_i - S_i)^2}}{\sqrt{\sum_{i=1}^n (O_i - \bar{O})^2}} \right] \quad (6)$$

$$263 \quad P - bias = \left[ \frac{\sum_{i=1}^n (O_i - S_i) \times 100}{\sum_{i=1}^n O_i} \right] \quad (7)$$

264 where  $O_i$  is the observed data at time step  $i$ , and  $S_i$  is the simulated output at time step  $i$ ,  $\bar{O}$  is  
 265 the mean of observed data over all time steps, and  $n$  is the total number of observed data. In  
 266 addition, the 95 percent prediction uncertainty (95 PPU) band was computed to evaluate model  
 267 uncertainty (Singh et al., 2014). The 95 PPU is computed as the range of values between top and  
 268 bottom 2.5 % of the cumulative distribution of simulation outputs obtained during the calibration  
 269 process.

270 [Insert Table 3. List of calibrated parameters]

271

## 272 **2.5 Climate sensitivity and change scenarios**

273 To evaluate the impacts of climate variability and change on watershed hydrological  
 274 processes, climate sensitivity and change scenarios were prepared as illustrated below (see 2.5.1



275 and 2.5.2). The calibrated SWAT model was simulated using climate sensitivity and change  
276 scenarios for comparison with baseline water and nitrate budgets.

277

### 278 **2.5.1 Climate sensitivity scenarios**

279 A climate sensitivity analysis aids in identifying the degree or threshold of responses of  
280 hydrologic variables to climate-induced modifications and a sensitivity scenario generally  
281 assumes constant changes throughout the year (Mearns, 2001). Following the approach in  
282 Mearns (2001), six climate sensitivity scenarios were prepared by modifying the baseline data  
283 (1999 – 2014) to assess individual effects of elevated CO<sub>2</sub> concentration, precipitation and  
284 temperature on watershed hydrological processes (Table 4). Sensitivity scenarios were designed  
285 to change one variable while holding other variables constant throughout the simulations.  
286 Baseline precipitation and temperature were modified by percent and absolute changes using  
287 anomaly and absolute data, respectively, as illustrated in Najjar et al. (2009). They reported  
288 mean temperature and precipitation changes over the CB for three future periods (2010 – 2039,  
289 2040 – 2069, and 2070 – 2099) relative to the baseline period (1971 – 2000) based on GCM  
290 outputs (Najjar et al., 2009). Baseline CO<sub>2</sub> concentration was set as the default value (330 ppm)  
291 for SWAT simulations. For the first and second scenarios, baseline CO<sub>2</sub> concentration was  
292 replaced with 590 and 850 ppm, respectively. The upper value of 850 ppm was used because  
293 GCMs used for temperature and precipitation sensitivity scenarios were forced under the  
294 Intergovernmental Panel on Climate Change (IPCC) Special Report on Emissions Scenarios  
295 (SRES) A2 scenario, assuming to reach CO<sub>2</sub> concentration of 850 ppm by the end of this century  
296 (Najjar et al., 2009). The lower value of 590 ppm (the average of 330 and 850 ppm) was  
297 considered to be the level of CO<sub>2</sub> concentration around the middle of this century.



298 [Insert Table 4. Climate sensitivity scenarios developed by modifying baseline values]

299

### 300 **2.5.2 Climate change scenario**

301 A GCM-based scenario is the most commonly used method for assessing future climate  
302 change impact (Mearns, 2001). We downloaded projected climate data (e.g., daily precipitation  
303 and maximum and minimum temperature) from the World Climate Research Program (WCRP;  
304 bias corrected and downscaled) and the Coupled Model Intercomparison Project3 (CMIP3)  
305 climate projection archive ([http://gdo-dcp.ucllnl.org/downscaled\\_cmip3\\_projections/](http://gdo-dcp.ucllnl.org/downscaled_cmip3_projections/)). Five  
306 GCM data under the IPCC SRES A2 scenario were downloaded (Table A2), because the A2  
307 scenario indicates the highest value of CO<sub>2</sub> concentration among available CO<sub>2</sub> emission  
308 scenarios in CMIP3. To be consistent with the period of the baseline data (1999 – 2014), 16-  
309 year future data (2083 – 2098) including a 2-year warm-up period were used. Similar to the  
310 baseline scenario, humidity, wind speed, and solar radiation values were generated using the  
311 SWAT built-in weather generator owing to data unavailability. We assumed CO<sub>2</sub> concentration  
312 for the future period as 820 ppm, as that is a specified CO<sub>2</sub> concentration under SRES A2  
313 scenario in CMIP3 (Meehl et al., 2007). We compared simulated water and nitrate budgets from  
314 the baseline simulation with the ensemble mean of those from simulations with five GCMs  
315 because substantial variations existed among the GCM projections (Shrestha et al., 2012; Van  
316 Liew et al., 2012). The range of changes in simulated outputs was represented with the ensemble  
317 mean to show overall responses of watershed hydrological processes to climate change (Shrestha  
318 et al., 2012; Van Liew et al., 2012).

319



## 320 **2.6 Analyses of simulation outputs**

321 Simulated outputs were summarized at multiple temporal scales (e.g., monthly, seasonal,  
322 and annual). Annual averages of stream flow, ET, and nitrate loads were calculated to  
323 investigate changes in water and nitrate budgets in response to climate sensitivity and change  
324 scenarios. The response of crop growth to climate variability and change was also analyzed to  
325 show the effects of modified crop biomass on hydrology and N cycle. For comparative analyses  
326 between two watersheds, simulated outputs were summarized seasonally for climate sensitivity  
327 scenarios (i.e., summer (April – September) and winter (October – March)) and monthly for the  
328 climate change scenario. Water and nitrate yields were calculated to identify key landscape  
329 characteristics greatly affecting nitrate loads under climate sensitivity scenarios. Note that water  
330 and nitrate yields indicate the summations of water and nitrate fluxes transported from lands to  
331 streams by surface runoff, lateral flow, and groundwater flow. All simulation outputs were  
332 normalized by total watershed size.

333 We conducted two statistical analyses to demonstrate whether significant differences  
334 existed between simulation outputs by climate conditions (baseline vs. climate sensitivity and  
335 change scenarios) and watershed characteristics (TCW vs. GW). Two t-tests widely used for  
336 demonstrating significant effects of climate change and study site characteristics on hydrologic  
337 variables (e.g., water and nitrate budgets) were utilized in this study (Ficklin et al., 2010 and  
338 2013; Lee et al., 2016). A paired sample t-test was performed to compare outputs from climate  
339 sensitivity and change scenarios to the baseline scenario at individual watersheds. A two-sample  
340 t-test was used to determine whether the differences between the two watersheds were significant.

341



342 **3 Results and Discussions**

343 **3.1 Model calibration and validation**

344 Monthly simulations for stream flow and nitrate loads were compared with corresponding  
345 observations (Figure 3). Results show that simulated monthly stream flow were in good  
346 agreement with observations, but simulated peak stream flows were underestimated relative to  
347 observations. This underestimation was attributed to the inherent limitations of SWAT model; it  
348 does not account for intensity and duration of the precipitation (Qiu et al., 2012). Previous  
349 studies conducted in this region have also predicted peak flows beyond the uncertainty band  
350 mainly due to model limitation, though the overall simulation results well replicated the actual  
351 observations (Yeo et al., 2014; Lee et al., 2016). Simulated nitrate loads were also well matched  
352 well actual observations and the uncertainty band (shown as green in Figure 3) captured most  
353 observations in the two watersheds. Overall, model performance measures fulfilled “good” or  
354 “very good” criteria for stream flow and at least “satisfactory” for nitrate loads (Table 5). These  
355 results demonstrated that the calibrated model replicated actual conditions reasonably well, and it  
356 was able to predict hydrologic variables under different modeling scenarios (Moriassi et al., 2007;  
357 Arnold et al. 2012).

358 [Insert Figure 3. Simulated and observed monthly stream flow and nitrate loads for (a & b) TCW  
359 and (c & d) GW during calibration and validation periods]

360 [Insert Table 5. Model performance measures for monthly stream flow and nitrate loads]

361



## 362 **3.2 Responses to climate sensitivity scenarios**

### 363 **3.2.1 Water and nitrate budgets**

364 14-year averages of annual hydrologic variables under the baseline and climate  
365 sensitivity scenarios are represented in Figure 4. Elevated CO<sub>2</sub> concentration (590 and 850 ppm)  
366 and precipitation increase (11 and 21 %) led to significant increases in annual stream flow and  
367 nitrate loads by 50 % and 52 % for TCW and 43 % and 33 % for GW, respectively, relative to  
368 the baseline scenario (*p-value* < 0.01) (Figure 4). Elevated CO<sub>2</sub> concentration lowered plant's  
369 stomatal conductance, resulting in a decrease in ET of 30 % and thereby increases in stream flow  
370 and nitrate loads (Figure 4). Precipitation increase resulted in a direct increase in stream flow,  
371 leading to increased nitrate loads. Compared to the baseline scenario, a temperature increase of  
372 5 °C significantly reduced annual stream flow and nitrate loads by 12 % and 13 % for TCW and  
373 11 and 13 % for GW (*p-value* < 0.01), respectively, due to intensified ET (Figure 4).

374 Changes in crop growth under climate sensitivity scenarios had great impacts on water  
375 and nitrate budgets. Although precipitation increase resulted in the greatest increase in annual  
376 stream flow, annual nitrate loads were greater under elevated CO<sub>2</sub> concentration (Figure 4ab),  
377 due to increased crop biomass (Figure 5a). Elevated CO<sub>2</sub> concentration stimulated crop growth  
378 by decreasing water demand and increasing radiation use efficiencies (Abler and Shortle, 2000;  
379 Parry et al., 2004). For example, simulated corn and soybean biomass increased from 1.5 and  
380 0.9 (baseline concentration of 330ppm) to 1.6 and 1.3 (CO<sub>2</sub> concentration of 850 ppm) Mg·ha<sup>-1</sup>,  
381 respectively (Figure 5a). Increased crop biomass left greater residue, which contributed to  
382 increasing nitrate level through mineralization (Lee et al., 2016). Our simulation results  
383 indicated that mineralized nitrate under elevated CO<sub>2</sub> concentration increased by 16 % for TCW  
384 and 15 % for GW, compared to the baseline values (Figure A3). Increased crop residue resulted



385 in greater nitrate loads under elevated CO<sub>2</sub> concentration in comparison to precipitation increase.

386 In contrast, temperature increase led to lower crop biomass than the baseline value, due to

387 increased heat stress (Figure 5b). Lower biomass reduced remaining crop residue and

388 subsequently reduced mineralized nitrate by 15 % compared to the baseline value. Reduction of

389 mineralized nitrate contributed to decreased nitrate loads in conjunction with intensified ET.

390 [Insert Figure 4. 14-year average of annual hydrologic variables under the baseline and climate

391 sensitivity scenarios at the watershed scale]

392 [Insert Figure 5. The responses of crop biomass growth to elevated CO<sub>2</sub> concentration,

393 temperature increases]

394

### 395 **3.2.2 Comparative analyses**

396 For the purpose of comparing the two watersheds in response to climate sensitivity

397 scenarios, 14-year averages of seasonal water and nitrate yields were calculated (Figure 6). Both

398 elevated CO<sub>2</sub> concentration and precipitation increase led to greater water and nitrate yields for

399 the two watersheds during winter and summer seasons, compared to the baseline scenario.

400 However, the seasonal pattern of nitrate yield differed between the two watersheds. Wintertime

401 water yield was greater than summertime value for both watersheds, which was consistent with

402 the seasonal pattern of nitrate yield for GW. However, summertime nitrate yield was greater

403 than wintertime value for TCW. This was because of the difference in percent agricultural lands

404 between TCW (54.0 %) and GW (36.1 %). Increased water yield could accelerate the export of

405 nitrate added to the watersheds through fertilizer activities mainly occurred during summer

406 seasons. Accordingly, increased water yield caused by elevated CO<sub>2</sub> concentration and



407 precipitation increase induced considerable increase in summertime nitrate yield by ~ 62.5 % for  
408 TCW, while moderately increasing it by ~ 35.6 % for GW, which is dominated by forest instead  
409 of croplands, when compared with the baseline values.

410 [Insert Figure 6. 14-year average of seasonal hydrologic variables under the baseline and climate  
411 sensitivity scenarios at the watershed scale]

412 Temperature increase reduced summertime water and nitrate yields by 18.5 % and 27 %  
413 for TCW and 13.9 % and 20.2 % for GW, respectively, mainly due to increased water loss by ET  
414 (Figure 6). Wintertime water yield also decreased for the two watersheds, but changes in  
415 wintertime nitrate yield differed between two them. A decrease of 9.5 % in wintertime nitrate  
416 yield was found for GW, but wintertime nitrate yield increased by 1.6 % for TCW (Figure 6b),  
417 due to modified crop growth patterns and contrasting soil characteristics between the two  
418 watersheds. Temperature increase most likely drove summer crops to reach maturity earlier than  
419 the baseline (Figure 5b). Once mature, the crops stopped consuming soil water and nitrate,  
420 subsequently increasing soil water content and nitrate leaching (Figure A4). Nitrate leached into  
421 groundwater was discharged to streams through groundwater flow during winter seasons. TCW  
422 showed increased nitrate leaching of  $1.0 \text{ kg N}\cdot\text{ha}^{-1}$  compared to GW, due to a higher rate of soil  
423 infiltration. Different leaching rates between TCW and GW soils led to a greater increase in  
424 wintertime nitrate flux transported by groundwater flow (NGWQ) for TCW ( $0.21 \text{ kg N}\cdot\text{ha}^{-1}$ )  
425 compared to GW ( $0.16 \text{ kg N}\cdot\text{ha}^{-1}$ ) (Figure 6b). However, intensified ET reduced wintertime  
426 water flux transported by surface runoff (SURQ) and nitrate flux transported by surface runoff  
427 (NSURQ) for the two watersheds. Because the majority of water fluxes was transported by  
428 groundwater flow for TCW and surface runoff for GW (Figure 6a), a decrease in SURQ led to a  
429 substantial reduction of wintertime NSURQ for GW ( $0.45 \text{ kg N}\cdot\text{ha}^{-1}$ ) and less reduction for



430 TCW ( $0.12 \text{ kg N}\cdot\text{ha}^{-1}$ ), compared to the baseline (Figure 6b). Therefore, both increased NGWQ  
431 and decreased NSURQ during winter seasons collectively led to an increasing pattern of  
432 wintertime nitrate yield for TCW and a decreasing pattern for GW, compared to the baseline  
433 scenario.

434

### 435 **3.3 Responses to the climate change scenario**

#### 436 **3.3.1 Comparison of climate data (baseline vs. climate change scenario)**

437 The monthly averages of mean temperature and cumulative precipitation under the  
438 baseline scenario were compared with the ensemble means of five GCMs (Figure 7). Projected  
439 temperature was constantly higher than the baseline value throughout the year with the increase  
440 rate of  $3.8 - 5.5 \text{ }^\circ\text{C}$  (Figure 7a). Compared to the baseline, projected precipitation was greater  
441 from January to March, but lower or similar during other months (Figure 7b). Monthly  
442 cumulative precipitation was up to 31 mm greater in January and up to 44 mm lower in October,  
443 in comparison to the baseline. Note that the annual average of mean temperature increased from  
444  $13.9 \text{ }^\circ\text{C}$  (baseline) to  $18.4 \text{ }^\circ\text{C}$  (projection), and the annual average of cumulative precipitation  
445 decreased from 1220 mm (baseline) to 1160 mm (projection).

446 [Insert Figure 7. Monthly average of (a) mean temperature and (b) cumulative precipitation for  
447 the baseline (2001 – 2014) and future (2083 – 2098) periods]

448

#### 449 **3.3.2 Water and nitrate budgets**

450 Baseline hydrologic variables (e.g., stream flow, ET, and nitrate loads) are compared  
451 with the ensemble means of simulated outputs in Table 6. Relative to the baseline scenario,



452 annual stream flow and nitrate loads significantly increased by 40 % and 39 % for TCW and 24 %  
453 and 24 % for GW ( $p$ -value < 0.01), respectively. These increasing patterns were mainly caused  
454 by decreased ET resulting from elevated CO<sub>2</sub> concentration of 820 ppm, considering that both  
455 precipitation decrease and temperature increase contributed to reducing stream flow and nitrate  
456 loads. Elevated CO<sub>2</sub> concentration reduced ET by 34 % for TCW and 32 % for GW (Table 6).  
457 In addition, warmer temperature led to the early maturity of crop biomass (Figure 8) and thereby  
458 early termination of water and nutrient uptake by crops, contributing to increasing stream flow  
459 and nutrient loads.

460 [Insert Table 6. 14-year average of hydrologic variables under the baseline and climate change  
461 scenarios]

462 [Insert Figure 8. Crop biomass growth under the baseline and climate change scenarios: (a) corn  
463 and (b) soybean]

464 It should be noted that the standard version of SWAT tends to overestimate the effect of  
465 CO<sub>2</sub> on the reduction of ET (Eckhardt and Ulbrich, 2003). Maximum leaf area index (LAI) is  
466 assumed to be constant regardless of variation in CO<sub>2</sub> concentration in SWAT. However,  
467 maximum LAI is known to increase with increasing CO<sub>2</sub> concentration (Eckhardt and Ulbrich,  
468 2003). In addition, the degree of reduction in stomatal conductance varies by plant species,  
469 which also is not taken into account in SWAT. Another model simplification, which increases  
470 uncertainty, is the application of the same reduction rate to all plants. For example, C3 crops  
471 (soybean and wheat) are known to have less reduction in stomatal conductance with rising CO<sub>2</sub>  
472 concentration compared to C4 crops (corn) (Ainsworth and Rogers, 2007). Both factors could  
473 contribute to overestimating the reduction of ET and resultant increase in stream flow and nitrate  
474 loads (Eckhardt and Ulbrich, 2003). Our results might overestimate CO<sub>2</sub> effects on streamflow



475 and nitrate loads relative to the effects of precipitation and temperature changes. However, this  
476 study attempted to demonstrate how watershed hydrological processes would respond to the  
477 combined effects of potential changes in CO<sub>2</sub> concentration, precipitation, and temperature.  
478 Therefore, our results provided feasible changes in water and nitrate budgets under potential  
479 climate change.

480

### 481 **3.3.3 Comparative analysis**

482 Responses of the two watersheds to the climate change scenario were compared using the  
483 monthly averages of water and nitrate yields in Figure 9. Relative to the baseline, projected  
484 water yield was greater over the year with the range of relative change between 14 and 99 % for  
485 TCW; however GW showed a decrease in water yield by 14 % in June and 6 % in October,  
486 mainly due to different soil characteristics. For example, substantial reduction of precipitation  
487 on two months (June and October) greatly decreased SURQ for both watersheds (Figure 9ab).  
488 Surface runoff is the major water pathway in GW and therefore reduction of SURQ resulted in  
489 lower water yield compared to the baseline value on two months.

490 Projected nitrate yield was greater than the baseline value throughout the year for both  
491 watersheds. The increased rate of nitrate yield differed between TCW (0.24 – 0.87 kg N·ha<sup>-1</sup>)  
492 and GW (0.03 – 0.35 kg N·ha<sup>-1</sup>) due to contrasting land use and soil characteristics (Figure 9cd).  
493 First, the larger percentage of croplands in TCW led to considerable nitrate export derived from  
494 fertilizer activities compared to GW with less percent croplands. This was because increased  
495 water yield by elevated CO<sub>2</sub> concentration and precipitation increase promoted the export of  
496 nitrate in soil profile. For example, nitrate yield increased by 0.87 kg N·ha<sup>-1</sup> for TCW and 0.35  
497 kg N·ha<sup>-1</sup> for GW in April, when fertilizer application occurred, compared to the baseline.



498 Second, different soil characteristics resulted in greater reduction of nitrate yield in GW and less  
499 in TCW in response to precipitation decrease in and temperature increase. Due to contrasting  
500 soil characteristics, the major nitrate transport occurred by groundwater flow for TCW and  
501 surface runoff for GW. Therefore, precipitation decrease and temperature increased that greatly  
502 reduced SURQ led to a greater reduction of NSURQ for GW ( $0.6 \text{ kg N}\cdot\text{ha}^{-1}$ ) than for TCW ( $0.1$   
503  $\text{kg N}\cdot\text{ha}^{-1}$  over the year. Note that NGWQ increased for both watersheds due to elevated  $\text{CO}_2$   
504 concentration. Lastly, increased nitrate loss by denitrification contributed to lower nitrate yield  
505 in GW (dominated by poorly-drained soils) where higher denitrification is expected, compared to  
506 TCW (dominated by well-drained soils). Increased soil water content by elevated  $\text{CO}_2$   
507 concentration provided conducive conditions (i.e., anaerobic) for denitrification. Compared to  
508 the baseline, GW and TCW showed increased nitrate (removed by denitrification) of 3.5 and 0.3  
509  $\text{kg N}\cdot\text{ha}^{-1}$  under the climate change scenario, respectively. Eventually, GW lost  $8.5 \text{ kg N}\cdot\text{ha}^{-1}$   
510 more nitrate flux via denitrification than TCW under the climate change scenario.

511 [Insert Figure 9. 14-year average of monthly water and nitrate yields under the baseline and  
512 climate change scenarios]

513

#### 514 **4 Implication**

515 The key results of this study can suggest important future tasks towards improving our  
516 understanding of climate change impacts on nutrient loads into the CBW. Analysis of climate  
517 variability and change impacts on watershed hydrological processes illustrated the close  
518 relationship between agricultural activities and future nitrate export in the watershed dominated  
519 by croplands, due to excessive export of nitrate from fertilizer application. Changes in crop



520 growth are likely to alter current agricultural activities and associated nitrate loads. Under the  
521 climate change scenario, maximum summer crop biomass decreased and the growth cycle of  
522 summer crops was shortened due to warmer temperature (Figure 8). To adapt to warmer  
523 temperature, early planting of summer crops could be suggested to increase crop production in  
524 the future. For example, when planting dates were shifted 10 days earlier, corn and soybean  
525 yields increased on average of 0.01 and 0.04 Mg·ha<sup>-1</sup> (Figure 8). Woznicki et al. (2015) also  
526 predicted that planting 10 days earlier contributes to increasing corn yield in southwest Michigan  
527 under climate change. However, early planting and associated fertilizer application might lead to  
528 increased nitrate export because increased precipitation during early spring could result in  
529 considerable export of nitrate from fertilizer application. In addition, fertilizer use would  
530 increase in the future due to reduced corn yield compared to the baseline (Figure 8), which  
531 potentially increases nitrate loads. Less water demand caused by elevated CO<sub>2</sub> concentration  
532 might require less irrigation demand. Therefore, it is crucial to investigate potential agricultural  
533 activities under climate change to accomplish targeted crop yield (e.g., shift of planting date and  
534 fertilizer addition) and their effects on nitrate loads.

535 Climate change-driven modifications indicated a potential overall increase in nitrate  
536 export. Therefore, the importance of conservation practices aimed at N mitigation would be  
537 even more critical in the future. Comparative analyses of hydrological processes between two  
538 watersheds with different physical characteristics provided insights regarding effective water  
539 quality management under climate change. The control of nutrients in manure or fertilizer would  
540 be more critical for reducing nitrate export from a watershed dominated by croplands where  
541 nitrate loads substantially increased under climate change, due to fertilizer application. Winter  
542 cover crops would be more valuable to mitigate agricultural nitrate yield during winter seasons,



543 considering the projected increase in future wintertime precipitation. In a watershed dominated  
544 by poorly-drained soils, wetland restoration would be well positioned to enhance denitrification  
545 (McCarty et al., 2014). In addition, the conservation/maintenance of prior converted croplands is  
546 also necessary for increased nitrate loss by denitrification. However, there is still a great  
547 uncertainty regarding whether current conservation practices would be adequate to mitigate  
548 increased nitrate loads by climate change (Woznicki and Nejadhashemi, 2012). The  
549 performance of conservation practices under climate change conditions should be further  
550 examined.

551

## 552 **5 Summary and Conclusion**

553 Water quality degradation by human activities on agricultural lands is a great concern in the  
554 Coastal Plain of the CBW. This degradation is expected to worsen in the future under climate  
555 variability and change. However, there is limited information about how climate change will  
556 influence hydrology and nutrient cycles. This study used SWAT model to simulate the impacts  
557 of potential climate variability and change on two adjacent watersheds in the Coastal Plain of the  
558 CBW. Climate sensitivity scenarios were developed to represent potential climate variability  
559 (e.g., increases in CO<sub>2</sub> concentration, precipitation, and temperature) based on the previous study  
560 (Najjar et al., 2009). Using five GCM data, the climate change scenario was prepared to depict  
561 future climate conditions. We performed comparative analyses between two watersheds to show  
562 how key landscape characteristics influence the watershed level response to climate variability  
563 and change.



564 Our simulation results showed that water and nitrate budgets in two watersheds in the Coastal  
565 Plain of the CBW were significantly sensitive to climate variability and change. Compared to  
566 the baseline scenario, a precipitation increase of 21% and elevated CO<sub>2</sub> concentration of 850  
567 ppm resulted in increases in stream flow and nitrate loads of 50 % and 52 %, respectively. A  
568 temperature increase of 5.0 °C reduced stream flow and nitrate loads by 12 % and 13 %,  
569 respectively. Under the climate change scenario, annual stream flow and nitrate loads increased  
570 by 40 % and 39 %, respectively, compared to the baseline scenario. Contrasting land use and  
571 soil characteristics led to different patterns of nitrate yield between two watersheds. The  
572 watershed with a larger percent croplands indicated increased nitrate yield of 0.52 kg N·ha<sup>-1</sup>  
573 compared to the one with less percent croplands under the climate change scenario, due to  
574 increased export of nitrate derived from fertilizer. Nitrate flux transported via surface runoff  
575 (NSURQ) was more susceptible to precipitation and temperature changes, in comparison to  
576 nitrate flux transported via groundwater flow (NGWQ). Accordingly, the poorly-drained  
577 watershed, where NSURQ accounts for the majority of nitrate yield, indicated less increase in  
578 nitrate yield due to considerable reduction of NSURQ in response to precipitation decrease and  
579 temperature increase under the climate change scenario, compared to the well-drained one,  
580 where NGWQ accounts for the majority of nitrate yield. Increased nitrate loss by denitrification  
581 also contributed to less increase in nitrate yield in the watershed dominated by poorly-drained  
582 soils compared to one dominated by well-drained soil. Based on our results, we suggest that  
583 increased implementation of conservation practices, such as nutrient management planning,  
584 winter cover crops, and wetland restoration and enhancement, is necessary to mitigate variations  
585 in nitrate loads caused by climate change. These findings should help watershed managers and



586 regulators to establish climate change adaptation strategies for mitigating water quality

587 degradation in this region.

588

589

590

591

592

593

594

595

596

597

598

599

600

601

602

603

604



605 **Acknowledgement**

606 This research was supported by the US Department of Agriculture (USDA) Conservation Effects  
607 Assessment Project (CEAP), National Aeronautics and Space Administration (NASA) Land  
608 Cover and Land Use Change (LCLUC) Program (award no: NNX12AG21G), and US  
609 Geological Survey (USGS) Land Change Science Program.

610

611 *Disclaimer.* The USDA is an equal opportunity provider and employer. Any use of trade, firm, or  
612 product names is for descriptive purposes only and does not imply endorsement by the US  
613 Government. The findings and conclusions in this article are those of the author(s) and do not  
614 necessarily represent the views of the U.S. Fish and Wildlife Service.

615

616

617

618

619

620

621

622

623

624



625 **References**

626 Abler, D.G. and Shortle, J.S.: Climate change and agriculture in the Mid-Atlantic  
627 Region. *Climate Res.*, 14 (3), 185-194, 2000.

628 Ainsworth, E.A. and Rogers, A.: The response of photosynthesis and stomatal conductance to  
629 rising [CO<sub>2</sub>]: mechanisms and environmental interactions. *Plant Cell Environ.*, 30(3),  
630 258-270, 2007.

631 Arnold, J.G., Moriasi, D.N., Gassman, P.W., Abbaspour, K.C., White, M.J., Srinivasan, R.,  
632 Santhi, C., Harmel, R.D., Van Griensven, A., Van Liew, M.W. and Kannan, N.: SWAT:  
633 Model use, calibration, and validation. *T. ASABE.*, 55(4), 1491-1508, 2012.

634 Ator, S.W. and Denver, J.M.: Estimating Contributions of Nitrate and Herbicides from  
635 Groundwater to Headwater Streams, Northern Atlantic Coastal Plain, United States. *J.*  
636 *Am. Water Resour. As.*, 48(6), 1075-90, 2012.

637 Chaplot, V.: Water and soil resources response to rising levels of atmospheric CO<sub>2</sub>  
638 concentration and to changes in precipitation and air temperature. *J. Hydrol.* 337(1), 159-  
639 171, 2007.

640 Chesapeake Bay Program: <http://www.chesapeakebay.net/discover/bay101/facts>, last access: 31  
641 May 2016

642 Chiang, S.L.: A runoff potential rating table for soils. *J. Hydrol.* 13, 54-62, 1971.

643 Denver, J.M., Tesoriero, A.J., and Barbaro, J.R.: Trends and Transformation of Nutrients and  
644 Pesticides in a Coastal Plain Aquifer System, United States. *J. Environ. Qual.* 39(1), 154-  
645 67, 2010.



- 646 Denver, J. M., Ator, S. W., Lang, M. W., Fisher, T. R., Gustafson, A. B., Fox, R., Clune, J. W.,  
647 and McCarty, G. W.: Nitrate fate and transport through current and former depressional  
648 wetlands in an agricultural landscape, Choptank Watershed, Maryland, United States. *J.*  
649 *Soil Water Conser.* 69 (1), 1-16, 2014.
- 650 Eckhardt, K. and Ulbrich, U.: Potential impacts of climate change on groundwater recharge and  
651 streamflow in a central European low mountain range. *J. Hydrol.* 284(1), 244-252, 2003.
- 652 Ficklin, D.L., Luo, Y., Luedeling, E., and Zhang, M.: Climate change sensitivity assessment of a  
653 highly agricultural watershed using SWAT. *J. Hydrol.* 374 (1), 16-29, 2009.
- 654 Ficklin, D.L., Luo, Y., Luedeling, E., Gatzke, S.E., and Zhang, M.: Sensitivity of agricultural  
655 runoff loads to rising levels of CO<sub>2</sub> and climate change in the San Joaquin Valley  
656 watershed of California. *Environ. Pollut.* 158 (1), 223-234, 2010.
- 657 Ficklin, D.L., Stewart, I.T., and Maurer, E.P.: Climate change impacts on streamflow and  
658 subbasin-scale hydrology in the upper Colorado River Basin. *PLOS ONE*, 8(8), e71297,  
659 2013.
- 660 Field, C.B., Jackson, R.B., and Mooney, H.A.: Stomatal responses to increased CO<sub>2</sub>:  
661 implications from the plant to the global scale. *Plant, Cell & Environment*, 18(10), 1214-  
662 1225, 1995.
- 663 Fisher, T. R., Jordan, T. E., Staver, K. W., Gustafson, A. B., Koskelo, A. I., Fox, R. J., Sutton, A.  
664 J., Kana, T., Beckert, K. A., Stone, J. P., McCarty, G., and Lang, M.: The Choptank  
665 Basin in transition: intensifying agriculture, slow urbanization, and estuarine  
666 eutrophication, in: *Coastal Lagoons: critical habitats of environmental change*, edited by:  
667 Kennish, M. J. and Paerl, H. W., CRC Press, 135–165, 2010.



- 668 Gassman, P.W., Reyes, M.R., Green, C.H. and Arnold, J.G.: The soil and water assessment tool:  
669 historical development, applications, and future research directions. T. ASABE., 50(4),  
670 1211-1250, 2007.
- 671 Gitau, M.W., and Chaubey, I.: Regionalization of SWAT Model Parameters for Use in  
672 Ungauged Watersheds. Water. 2(4), 849-71, 2010.
- 673 Glancey, J., Brown, B., Davis, M., Towle, L., Timmons, J., and Nelson, J.: Comparison of  
674 Methods for Estimating Poultry Manure Nutrient Generation in the Chesapeake Bay  
675 Watershed, available at: [http://www.csgeast.org/2012annualmeeting/documents/  
676 Glancey.pdf](http://www.csgeast.org/2012annualmeeting/documents/Glancey.pdf) (last access: 25 September 2014), 2012.
- 677 Gombault, C., Madramootoo, C.A., Michaud, A., Beaudin, I., Sottile, M.F., Chikhaoui, M., and  
678 Ngwa, F.: Impacts of climate change on nutrient losses from the Pike River watershed of  
679 southern Québec. Can. J. of Soil Sci. 95(4), 337-358, 2015.
- 680 Hively, W.D., Hapeman, C.J., McConnell, L.L., Fisher, T.R., Rice, C.P., McCarty, G.W.,  
681 Sadeghi, A.M., Whittall, D.R., Downey, P.M., de Guzmán, G.T.N. and Bialek-Kalinski,  
682 K.: Relating nutrient and herbicide fate with landscape features and characteristics of 15  
683 subwatersheds in the Choptank River watershed. Sci. Total Environ. 409(19), 3866-3878,  
684 2011.
- 685 Howarth, R.W., Swaney, D.P., Boyer, E.W., Marino, R., Jaworski, N., and Goodale, C.: The  
686 influence of climate on average nitrogen export from large watersheds in the  
687 Northeastern United States. Biogeochemistry. 79(1-2), 163-186, 2006.



- 688 Jha, M., Arnold, J.G., Gassman, P.W., Giorgi, F. and Gu, R.R.: CLIMATE CHHANGE  
689 SENSITIVITY ASSESSMENT ON UPPER MISSISSIPPI RIVER BASIN  
690 STREAMFLOWS USING SWAT1. *J. Am. Water Resour. As.*, 997-1015, 2006.
- 691 Jordan, T.E., Correll, D.L. and Weller, D.E.: Relating nutrient discharges from watersheds to  
692 land use and streamflow variability. *Water Resour. Res.* 33(11), 2579-2590, 1997.
- 693 Lee, S., Yeo, I.Y., Sadeghi, A.M., McCarty, G.W. and Hively, W.D.: Prediction of climate  
694 change impacts on agricultural watersheds and the performance of winter cover crops:  
695 Case study of the upper region of the Choptank River Watershed, Proceedings of  
696 the ASABE 1st Climate Change Symposium: Adaptation and Mitigation, Chicago, IL, 3-  
697 5, May 2015
- 698 Lee, S., Yeo, I.-Y., Sadeghi, A. M., McCarty, W. M., Hively, W. D., and Lang, M. W.: Impacts  
699 of Watershed Characteristics and Crop Rotations on Winter Cover Crop Nitrate Uptake  
700 Capacity within Agricultural Watersheds in the Chesapeake Bay Region. *PLOS ONE*.  
701 11(6), e0157637, 2016.
- 702 Luo, Y., Ficklin, D.L., Liu, X. and Zhang, M.: Assessment of climate change impacts on  
703 hydrology and water quality with a watershed modeling approach. *Sci. Total*  
704 *Environ.* 450, 72-82, 2013.
- 705 McCarty, G.W., McConnell, L.L., Hapeman, C.J., Sadeghi, A., Graff, C., Hively, W.D., Lang,  
706 M.W., Fisher, T.R., Jordan, T., Rice, C.P., and Codling, E.E.: Water quality and  
707 conservation practice effects in the Choptank River watershed. *J. Soil Water*  
708 *Conserv.* 63(6), 461-474, 2008.



- 709 McCarty, G.W., Hapeman, C.J., Rice, C.P., Hively, W.D., McConnell, L.L., Sadeghi, A.M.,  
710 Lang, M.W., Whitall, D.R., Bialek, K. and Downey, P.: Metolachlor metabolite (MESA)  
711 reveals agricultural nitrate-N fate and transport in Choptank River watershed. *Sci. Total*  
712 *Environ.* 473, 473-482, 2014.
- 713 Mearns, L.O., Hulme, M., Carter, T.R., Leemans, R., Lal, M., Whetton, P., Hay, L., Jones, R.N.,  
714 Kittel, T., Smith, J. and Wilby, R.: Climate scenario development, 2001.
- 715 Meehl, G.A., Covey, C., Delworth, T., Latif, M., McAvaney, B., Mitchell, J., Stouffer, R., and  
716 Taylor, K.: The WCRP CMIP3 multi-model dataset: A new era in climate change  
717 research. *B. Am. Meteorol. Soc.* 88, 1383-1394, 2007.
- 718 Moriasi, D. N., Arnold, J. G., Van Liew, M. W., Bingner, R. L., Harmel, R. D., and Veith, T. L.:  
719 Model evaluation guidelines for systematic quantification of accuracy in watershed  
720 simulations. *T. ASABE.* 50(3), 885-900, 2007.
- 721 Najjar, R., Patterson, L., and Graham, S.: Climate simulations of major estuarine watersheds in  
722 the Mid-Atlantic region of the US. *Climatic Change*, 95 (1-2), 139-168, 2009.
- 723 Najjar, R.G., Pyke, C.R., Adams, M.B., Breitburg, D., Hershner, C., Kemp, M., Howarth, R.,  
724 Mulholland, M.R., Paolisso, M., Secor, D. and Sellner, K.: Potential climate-change  
725 impacts on the Chesapeake Bay. *Estuar. Coast. Shelf S.* 86(1), 1-20, 2010.
- 726 Neitsch, S. L., Arnold, J. G., Kiniry, J. R., and Williams, J. R.: Soil and Water Assessment Tool.  
727 Theoretical Documentation; Version 2009, Texas Water Resources Institute Technical  
728 Report No. 406, Texas A&M University System, College Station, TX, 2011.



- 729 Parry, M.L., Rosenzweig, C., Iglesias, A., Livermore, M. and Fischer, G.: Effects of climate  
730 change on global food production under SRES emissions and socio-economic  
731 scenarios. *Global Environ. Chang.* 14(1), 53-67, 2004.
- 732 Praskievicz, S.: IMPACTS OF PROJECTED CLIMATE CHANGES ON STREAMFLOW  
733 AND SEDIMENT TRANSPORT FOR THREE SNOWMELT-DOMINATED RIVERS  
734 IN THE INTERIOR PACIFIC NORTHWEST. *River Res. Appl.* 2014.
- 735 Qiu, L., Zheng, F., and Yin, R.: SWAT-based runoff and sediment simulation in a small  
736 watershed, the loessial hilly-gullied region of China: capabilities and challenges. *Int. J.*  
737 *Sediment Res.* 27(2): 226-234, 2012.
- 738 Rogers, C.E. and McCarty, J.P.: Climate change and ecosystems of the Mid-Atlantic  
739 Region. *Climate Res.* 14(3), 235-244, 2000.
- 740 Runkel, R.L., Crawford, C.G. and Cohn, T.A., 2004. Load Estimator (LOADEST): A  
741 FORTRAN program for estimating constituent loads in streams and rivers. U.S.  
742 Geological Survey Paper, Reston, Virginia, 2004
- 743 Sexton, A.M., Sadeghi, A.M., Zhang, X., Srinivasan, R. and Shirmohammadi, A.: Using  
744 NEXRAD and rain gauge precipitation data for hydrologic calibration of SWAT in a  
745 northeastern watershed. *T. ASABE*, 53(5), 1501-1510, 2010.
- 746 Seo, M., Yen, H., Kim, M.K. and Jeong, J.: Transferability of SWAT Models between  
747 SWAT2009 and SWAT2012. *J. Environ Qual*, 43(3), 869-880, 2014.
- 748 Sharifi, A., Lang, M.W., McCarty, G.W., Sadeghi, A.M., Lee, S., Yen, H., Rabenhorst, M.C.,  
749 Jeong, J. and Yeo, I.Y.: Improving Model Prediction Reliability through Enhanced



- 750 Representation of Wetland Soil Processes and Constrained Model Auto Calibration–A  
751 Paired Watershed Study. *J. Hydrol*, 541, 1088-1103, 2016.
- 752 Shelton, D.R., Sadeghi, A.M. and McCarty, G.W.: Effect of soil water content on denitrification  
753 during cover crop decomposition. *Soil Sci.* 165(4), 365-371, 2000.
- 754 Shrestha, R.R., Dibike, Y.B. and Prowse, T.D.: Modelling of climate-induced hydrologic  
755 changes in the Lake Winnipeg watershed. *J. Great Lakes Res.* 38, 83-94, 2012.
- 756 Singh, A., Imtiyaz, M., Isaac, R.K. and Denis, D.M.: Assessing the performance and uncertainty  
757 analysis of the SWAT and RBNN models for simulation of sediment yield in the Nagwa  
758 watershed, India. *Hydrolog. Sci. J.* 59(2), 351-364, 2014.
- 759 Tiner, R. W., Burke, D. G.: *Wetlands of Maryland*. US Fish and Wildlife Service, Hadly,  
760 Massachusetts, 261 pp, 1995.
- 761 Uniyal, B., Jha, M.K. and Verma, A.K.: Assessing climate change impact on water balance  
762 components of a river basin using SWAT model. *Water Resour. Manag.* 29(13), 4767-  
763 4785, 2015.
- 764 Van Liew, M.W., Feng, S. and Pathak, T.B.: Climate change impacts on streamflow, water  
765 quality, and best management practices for the shell and logan creek watersheds in  
766 Nebraska, USA. *Int. J. Agric. Biol. Eng.* 5(1), 13-34, 2012.
- 767 Woznicki, S.A. and Nejadhashemi, A.P.: Sensitivity Analysis of Best Management Practices  
768 Under Climate Change Scenarios I. *J. Am. Water Resour. As.* 48(1), 90-112, 2012.
- 769 Woznicki, S.A., Nejadhashemi, A.P. and Parsinejad, M.: Climate change and irrigation demand:  
770 Uncertainty and adaptation. *J. Hydrol.: Regional Studies.* 3, 247-264, 2015.



771 Wu, Y., Liu, S. and Gallant, A.L.: Predicting impacts of increased CO<sub>2</sub> and climate change on  
772 the water cycle and water quality in the semiarid James River Basin of the Midwestern  
773 USA. *Sci. Total Environ.* 430, 150-160, 2012a.

774 Wu, Y., Liu, S. and Abdul-Aziz, O.I.: Hydrological effects of the increased CO<sub>2</sub> and climate  
775 change in the Upper Mississippi River Basin using a modified SWAT. *Climatic*  
776 *Change*, 110(3-4), 977-1003, 2012b.

777 Yeo, I.Y., Lee, S., Sadeghi, A.M., Beeson, P.C., Hively, W.D., McCarty, G.W. and Lang, M.W.:  
778 Assessing winter cover crop nutrient uptake efficiency using a water quality simulation  
779 model. *Hydrol. Earth Syst. Sc.* 18(12), 5239-5253, 2014.

780

781

782

783

784

785

786

787

788

789

790



791 **List of Tables**

792 **Table 1.** Soil properties and land use distribution of Tuckahoe Creek Watershed (TCW) and  
793 Greensboro Watershed (GW) (adapted from Lee et al. (2016))

794 **Table 2.** List of SWAT model input data

795 **Table 3.** List of calibrated parameters

796 **Table 4.** Climate sensitivity scenarios developed by modifying baseline values

797 **Table 5.** Model performance measures for monthly stream flow and nitrate loads

798 **Table 6.** 14-year average of hydrologic variables under the baseline and climate change  
799 scenarios

800

801

802

803

804

805

806

807

808



809 **Table 1.** Soil properties and land use distribution of Tuckahoe Creek Watershed (TCW) and  
 810 Greensboro Watershed (GW) (adapted from Lee et al. (2016))

Land use	TCW	GW
Agriculture	54.0 % [69.5% / 30.5 %]	36.1 % [32.8% / 67.2 %]
Forest	32.8 %	48.3 %
Pasture	8.4 %	9.3 %
Urban	4.2 %	5.6 %
Water body	0.6 %	0.7 %
Hydrologic soil groups (HSGs)	TCW	GW
A	0.3 %	3.1 %
B	55.8 %	22.4 %
C	2.2 %	4.2 %
D	41.7 %	70.3 %

811 Note: Values in parenthesis [], denote the proportion of well-drained soils (HSG-A&B) and  
 812 poorly-drained soils (HSG-C&D) used for agricultural lands, respectively.

813

814

815 **Table 2.** List of SWAT model input data

Data	Source	Description	Year
DEM	MD-DNR	LiDAR-based 2 meter resolution	2006
Land use	USDA-NASS	Cropland Data Layer (CDL)	2008 - 2012
	MRLC	National Land Cover Database (NLCD)	2006
	USDA-FSA-APFO	National Agricultural Imagery Program digital Orthophoto quad imagery	1998
	US Census Bureau	TIGER road map	2010
Soils	USDA-NRCS	Soil Survey Geographical Database (SSURGO)	2012
Climate	NCDC	Daily precipitation and temperature	1999 - 2014
Stream flow	USGS	Monthly stream flow	2001 - 2014
Water quality	USGS and CBP	Daily grab nitrate samples	2001 - 2014

816 Note: MD-DNR: Maryland Department of Natural Resources, USDA-NASS (National  
 817 Agricultural Statistics Service), MRLC: Multi-Resolution Land Characteristics Consortium,  
 818 USDA-NRCS (Natural Resources Conservation Service), USDA-FSA-APFO (Farm Service  
 819 Agency-Aerial Photography Field Office).

820

821

822

823



824 **Table 3.** List of calibrated parameters

Parameter	Variable	Description (unit)	Range	Calibrated value	
				TCW	GW
CN2 <sup>#</sup>		Curve number	-50 - 50 %	-30 %	0%
ESCO <sup>#</sup>		Soil evaporation compensation factor	0 - 1	1	0.95
SURLAG <sup>#</sup>		Surface runoff lag coefficient	0.5 - 24	0.5	0.5
SOL_AWC <sup>#</sup>		Available water capacity of the soil layer (mm H <sub>2</sub> O·mm soil <sup>-1</sup> )	-50 - 50 %	-10%	-1%
SOL_K <sup>#</sup>		Saturated hydraulic conductivity (mm·hr <sup>-1</sup> )	-50 - 50 %	50 %	49 %
SOL_Z <sup>#</sup>		Depth from soil surface to bottom of layer (mm)	-50 - 50 %	-20 %	-31 %
ALPHA_BF <sup>#</sup>	Stream flow	Base flow recession constant (1·days <sup>-1</sup> )	0 - 1	0.07	0.051
GW_DELAY <sup>#</sup>		Groundwater delay time (days)	0 - 500	120	45
GW_REVAP <sup>#</sup>		Groundwater “revap” coefficient	0.02 - 0.2	0.10	0.02
RCHRG_DP <sup>#</sup>		Deep aquifer percolation fraction	0 - 1	0.01	0.05
GWQMN <sup>#</sup>		Threshold depth of water in the shallow aquifer required for return flow to occur (mm)	0 - 5000	1.9	1.0
CH_K2 <sup>#</sup>		Effective hydraulic conductivity (mm·hr <sup>-1</sup> )	0 - 150	0	20
CH_N2 <sup>#</sup>		Manning coefficient	0.01 - 0.3	0.29	0.021
NPERCO <sup>†</sup>		Nitrogen percolation coefficient	0.01 - 1	0.5	0.2
N_UPDIS <sup>†</sup>		Nitrogen uptake distribution parameter	5 - 50	50	50
ANION_EXCL <sup>†</sup>		Fraction of porosity from which anions are excluded	0.1 - 0.7	0.59	0.6
ERORGN <sup>†</sup>	Nitrate	Organic N enrichment ratio for loading with sediment	0 - 5	4.92	4.1
BIOMIX <sup>†</sup>		Biological mixing efficiency	0.01 - 1	0.01	0.01
SOL_NO3 <sup>§</sup>		Initial NO <sub>3</sub> concentration in soil layer (mg N·kg <sup>-1</sup> )	0 - 100	11.23	0
CDN <sup>§</sup>		Denitrification exponential rate coefficient	0 - 3.0	0.3	1.8
SDNCO <sup>§</sup>		Denitrification threshold water content	0.1 - 1.1	1.0	1.0

825 \* refers to a default value. The ranges of parameters with superscripts (#, †, §, \$) were adapted  
 826 from Gitau and Chaubey (2010), Yeo et al. (2014), Seo et al. (2012), Neitsch et al. (2011),  
 827 respectively.

828

829

830

831

832 **Table 4.** Climate sensitivity scenarios developed by modifying baseline values

Scenario	Percent increase of precipitation (%)	Absolute increase of temperature (°C)	Replacement of CO <sub>2</sub> (ppm)
Baseline	0	0	330
1	0	0	590
2	0	0	850
3	11	0	330
4	21	0	330
5	0	2.9	330
6	0	5.0	330

833

834

835

836 **Table 5.** Model performance measures for monthly stream flow and nitrate loads

Period	Variable	Stream flow		Nitrate loads	
		TCW	GW	TCW	GW
Calibration	NSE	0.723**	0.686**	0.623*	0.702**
	RSR	0.523**	0.556**	0.610*	0.542**
	P-bias (%)	-5.8***	-3.2***	-9.8***	-4.1***
Validation	NSE	0.674**	0.790***	0.604*	0.567*
	RSR	0.566**	0.454***	0.624*	0.652*
	P-bias (%)	17.8**	13***	-5.6***	-12.1***

837 Model performances were rated based on the criteria of Moriasi et al. (2008); \* Satisfactory, \*\*  
838 Good, and \*\*\* Very Good; Satisfactory ( $0.5 < \text{NSE} \leq 0.65$ ,  $0.6 < \text{RSR} \leq 0.7$ , and  $\pm 15 \leq \text{P-bias} <$   
839  $\pm 25$ ), \*\* Good ( $0.65 < \text{NSE} \leq 0.75$ ,  $0.5 < \text{RSR} \leq 0.6$ , and  $\pm 10 \leq \text{P-bias} < \pm 15$ ), and \*\*\* Very  
840 Good ( $0.75 < \text{NSE} \leq 1.0$ ,  $0.0 < \text{RSR} \leq 0.5$ ,  $\text{P-bias} < \pm 10$ ).

841

842

843

844

845

846

847

848

849



850 **Table 6.** 14-year average of hydrologic variables under the baseline and climate change  
851 scenarios

Variables	TCW			GW		
	Baseline	Projection	Relative change (%)	Baseline	Projection	Relative change (%)
Stream flow ( $\text{m}^3 \cdot \text{s}^{-1} \cdot \text{ha}^{-1} \cdot 10^4$ )	1.5	2.1 (1.6 – 2.7)	40	1.7	2.1 (1.6 – 2.6)	24
ET ( $\text{mm} \cdot \text{ha}^{-1}$ )	2.7	1.8	-34	2.3	1.6	-32
Nitrate loads ( $\text{kg N} \cdot \text{ha}^{-1}$ )	12.5	17.5 (14.6 – 21.4)	39	5.3	6.6 (5.5 – 8.1)	24

852 Note: Projection stands for the ensemble mean of simulated hydrologic variables with 5 GCMs.  
853 The numbers within parenthesis indicates the maximum and minimum values of simulations with  
854 five GCM data. Relative change indicates the percent changes in the ensemble mean relative to  
855 the baseline value.

856

857

858

859

860

861

862

863

864

865

866

867



868 **List of Figures**

869 **Figure 1.** The location of Tuckahoe Creek Watershed (left) and Greensboro Watershed (right)

870 **Figure 2.** The physical characteristics of Tuckahoe Creek Watershed (left) and Greensboro  
871 Watershed (right); (a) land use, (b) hydrologic soil groups, and (c) elevation

872 **Figure 3.** Simulated and observed monthly stream flow and nitrate loads for (a & b) TCW and (c  
873 & d) GW during calibration and validation periods

874 **Figure 4.** 14-year average of annual hydrologic variables under the baseline and climate  
875 sensitivity scenarios at the watershed scale: (a) stream flow and evapotranspiration (ET), (b)  
876 nitrate loads, and (c) mineralized nitrate.

877 **Figure 5.** The responses of crop biomass growth to elevated CO<sub>2</sub> concentration, temperature  
878 increases: corn (a & b) and soybean (c & d). TMP in (b & d) stands for temperature.

879 **Figure 6.** 14-year average of seasonal hydrologic variables under the baseline and climate  
880 sensitivity scenarios at the watershed scale: (a) water and (b) nitrate yields.

881 **Figure 7.** Monthly average of (a) mean temperature and (b) cumulative precipitation for the  
882 baseline (2001 – 2014) and future (2083 – 2098) periods.

883 **Figure 8.** 14-year average of monthly water and nitrate yields under the baseline and climate  
884 change scenarios. The descriptions of abbreviation are illustrated in the caption of Figure 6.

885 **Figure 9.** Crop biomass growth under the baseline and climate change scenarios (projection): (a)  
886 corn and (b) soybean.

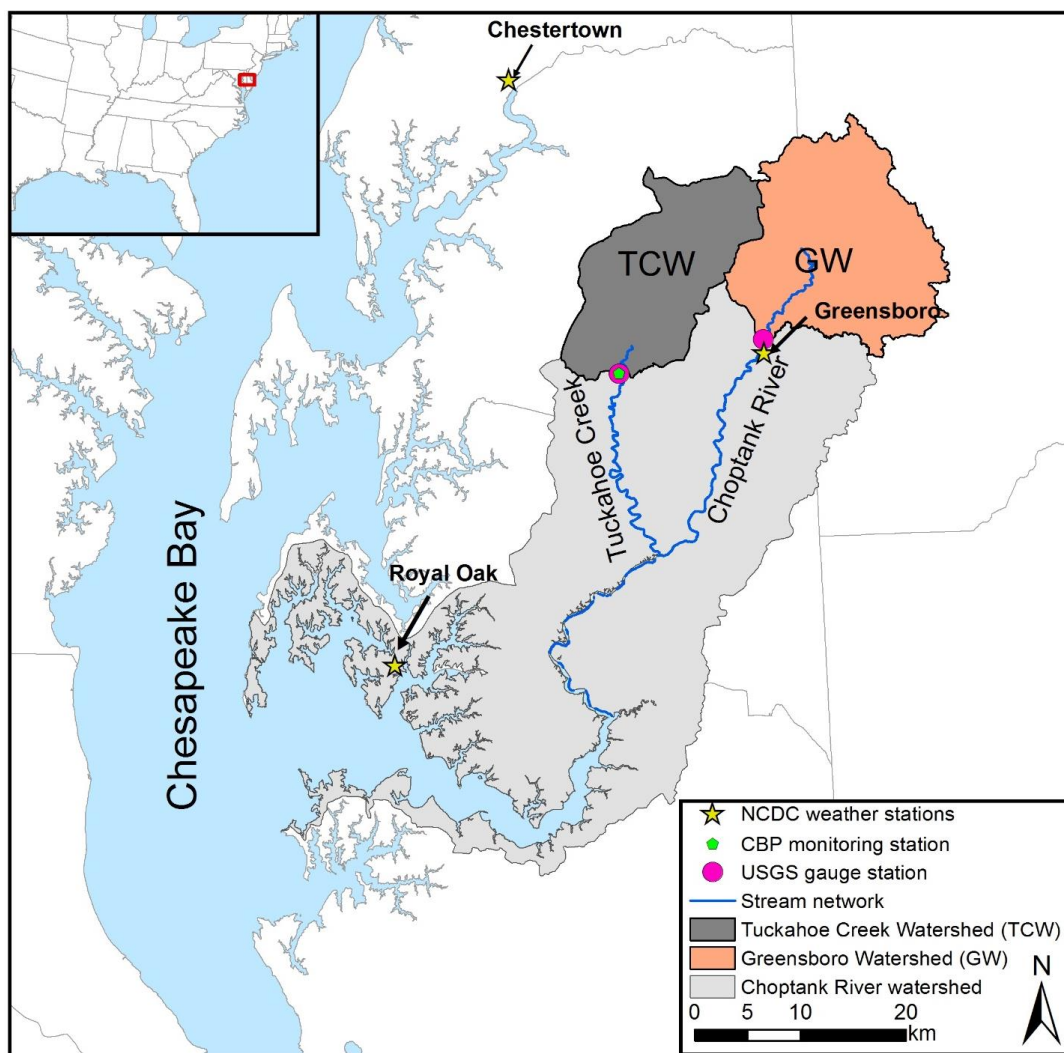
887

888

889

890

891



892

893 **Figure 1.** The location of Tuckahoe Creek Watershed (left) and Greensboro Watershed (right)  
894 (adapted from Lee et al. (2016))

895

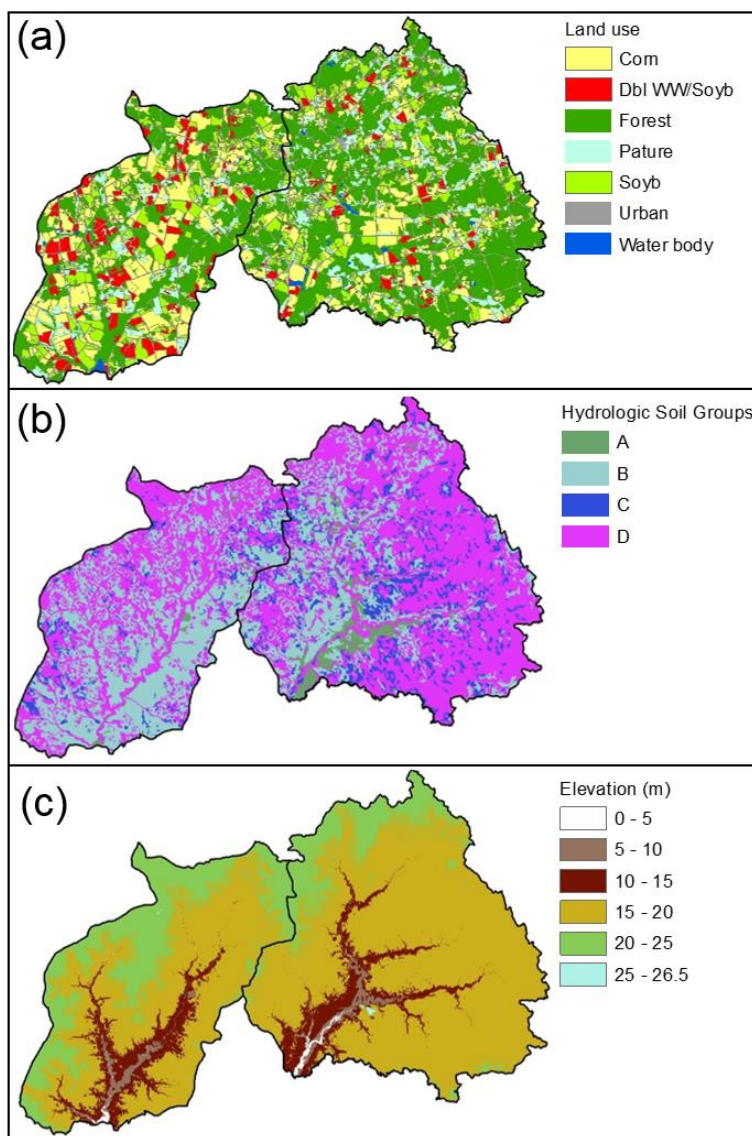
896

897

898

899

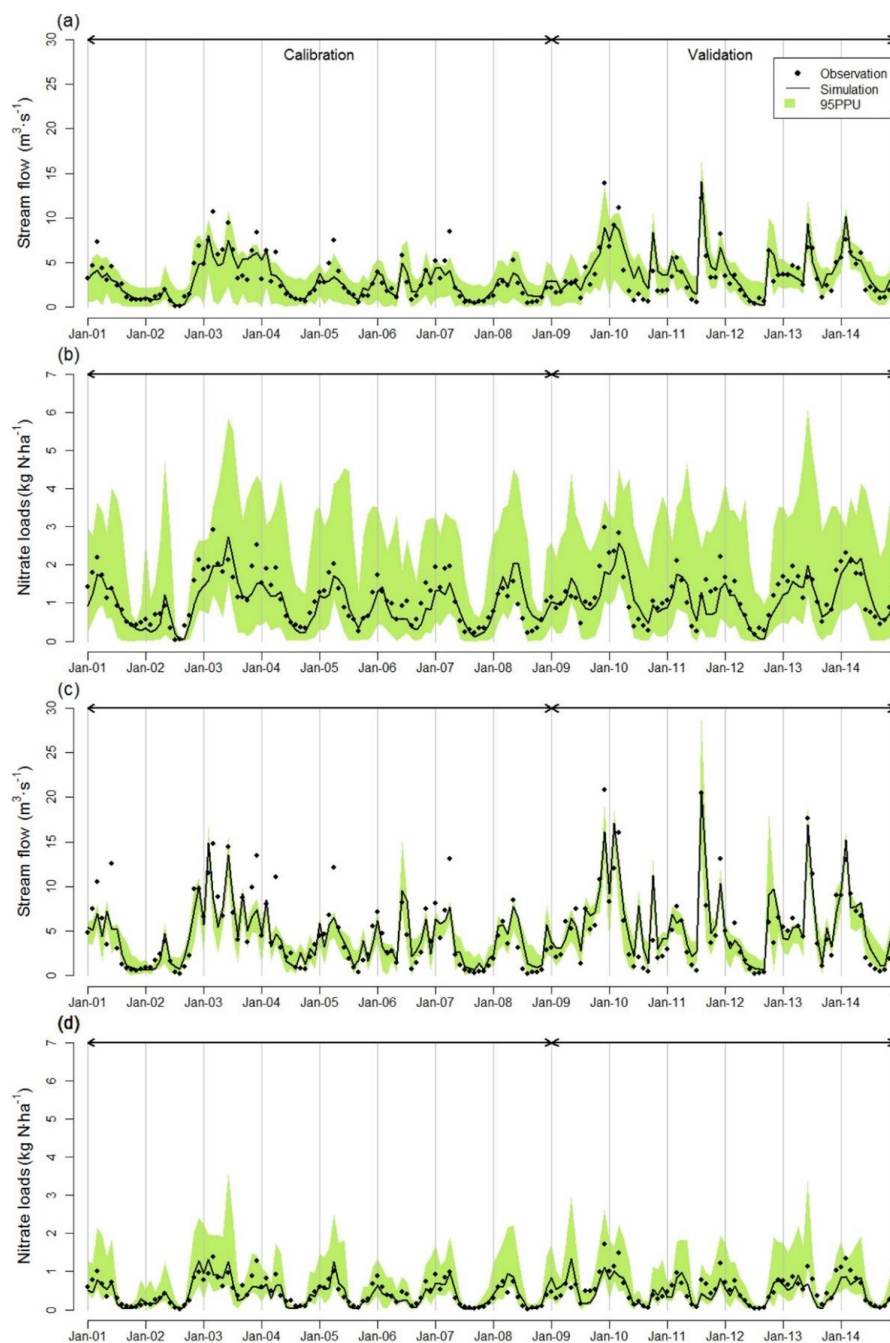
900



901

902 **Figure 2.** The physical characteristics of Tuckahoe Creek Watershed (left) and Greensboro  
903 Watershed (right); (a) land use, (b) hydrologic soil groups, and (c) elevation (adapted from Lee  
904 et al. (2016)).

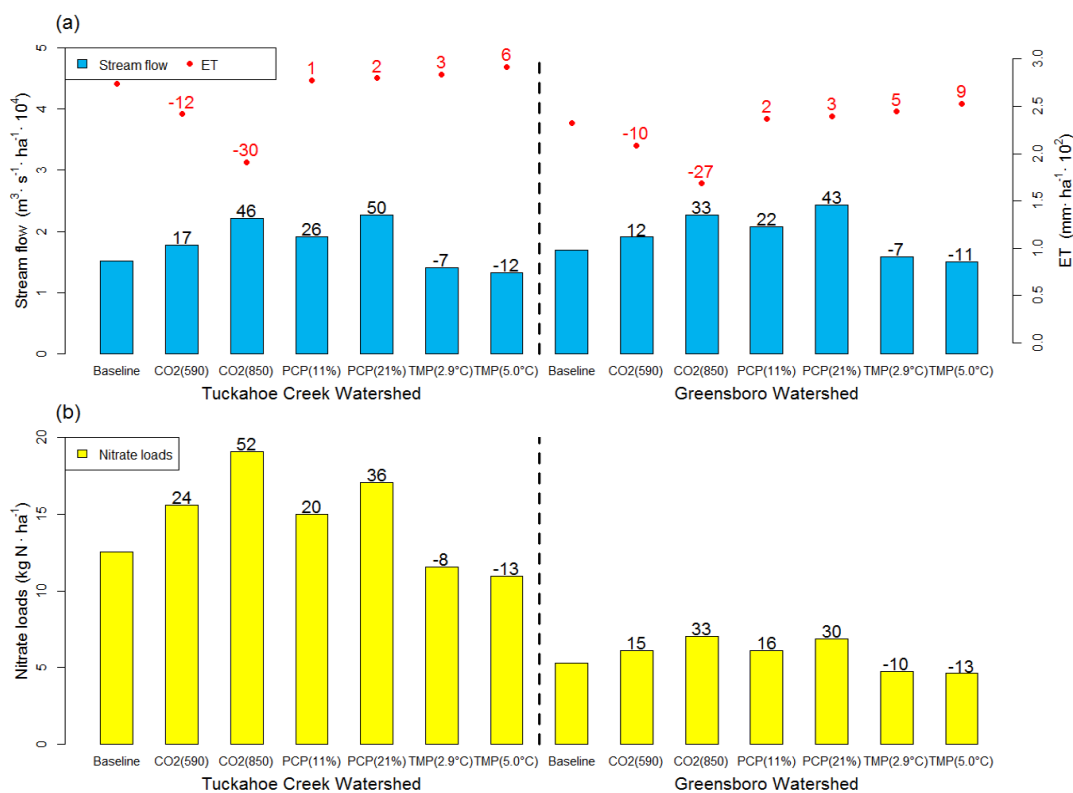
905 Note: Dbl WW/Soyb stands for double crops of winter wheat and soybean in a year. Hydrologic  
906 soil groups (HSGs) are characterized as follows: Type A- well-drained soils with 7.6-11.4 mm/hr  
907 (0.3-0.45 inch/hr) water infiltration rate; Type B - moderately well-drained soils with 3.8-7.6  
908 mm/hr (0.15-0.30 inch/hr) water infiltration rate; Type C - moderately poorly-drained soils with  
909 1.3-3.8 mm/hr (0.05-0.15 in/hr) water infiltration rate; Type D – poorly-drained soils with 0-1.3  
910 mm/hr (0-0.05 inch/hr) water infiltration rate (Netisch et al., 2011).



911

912 **Figure 3.** Simulated and observed monthly stream flow and nitrate loads for (a & b) TCW and (c  
913 & d) GW during calibration and validation periods.

914 Note: 95 PPU stands for 95 percent prediction uncertainty.



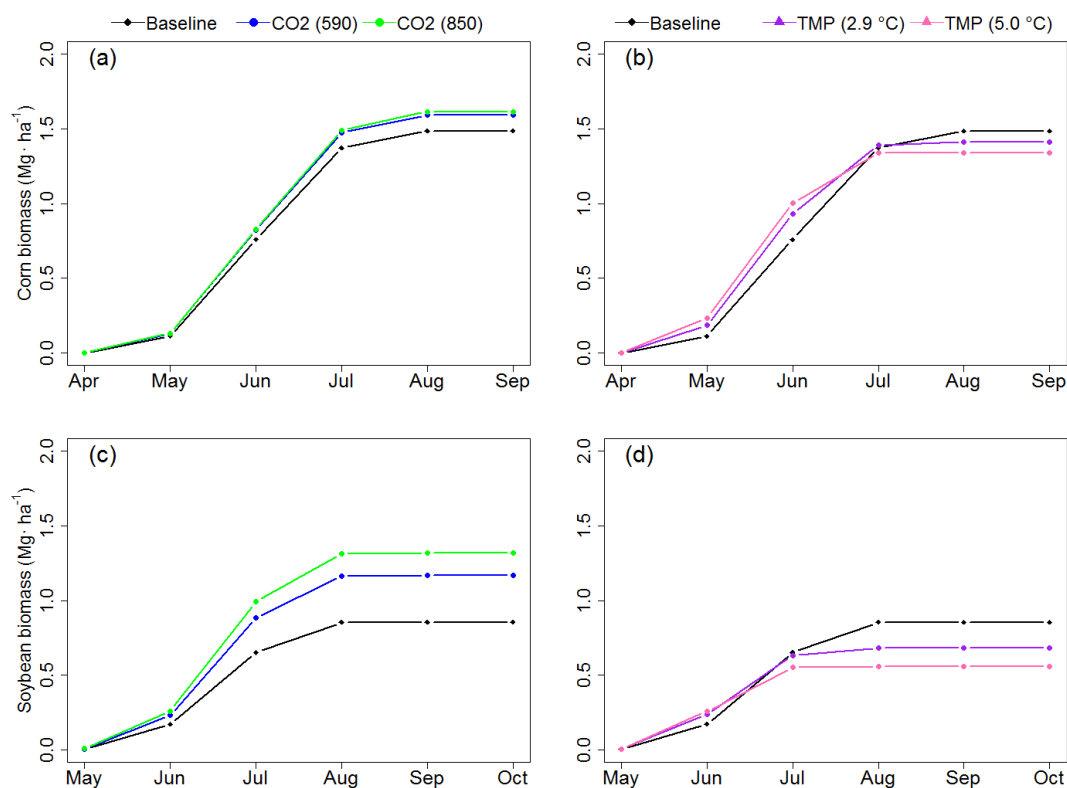
915

916 **Figure 4.** 14-year average of annual hydrologic variables under the baseline and climate  
 917 sensitivity scenarios at the watershed scale: (a) stream flow and evapotranspiration (ET), and (b)  
 918 nitrate loads.

919 Note: The red and black numerical values above the bar and the dot graphs, respectively, indicate  
 920 the relative changes (%) in hydrologic variables for climate sensitivity scenarios relative to the  
 921 baseline scenario [relative change (%) = (Sensitivity Scenarios – Baseline) / Baseline × 100].  
 922 PCP and TMP stand for precipitation and temperature, respectively.

923

924



925

926 **Figure 5.** The responses of crop biomass growth to elevated CO<sub>2</sub> concentration, temperature  
 927 increases: (a & b) corn and (c & d) soybean.

928 Note: TMP in the legend of (b) stands for temperature.

929

930

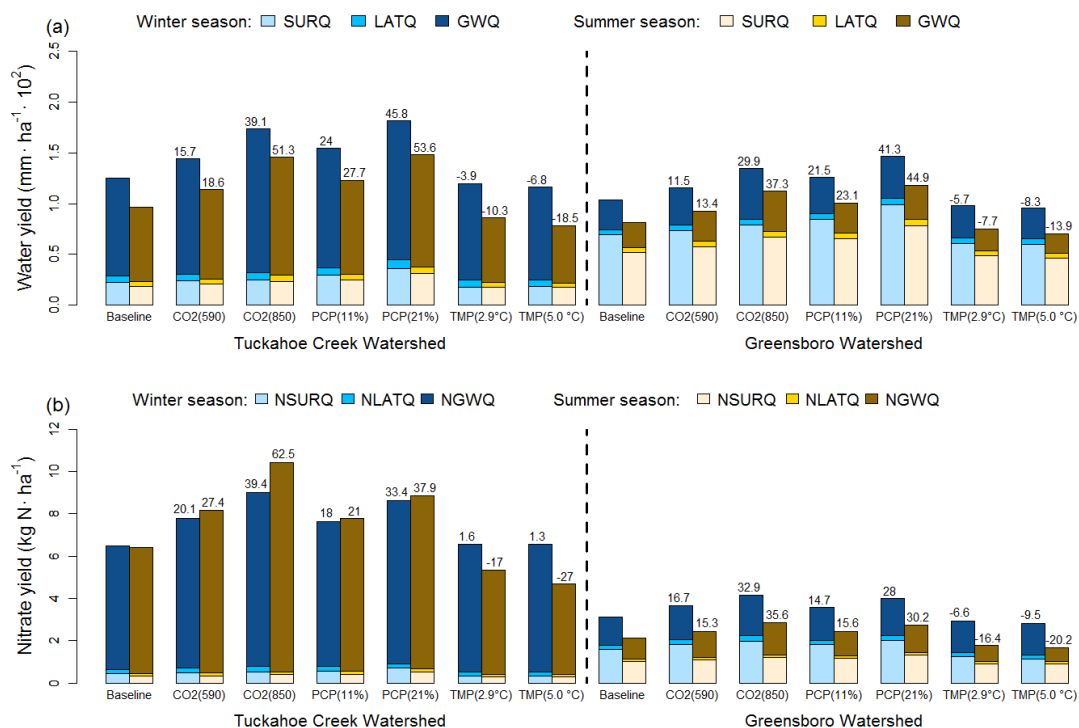
931

932

933

934

935



936

937 **Figure 6.** 14-year average of seasonal hydrologic variables under the baseline and climate  
 938 sensitivity scenarios at the watershed scale: (a) water and (b) nitrate yields.

939 Note: The number on the bar graph indicates the relative changes (%) in hydrologic variables for  
 940 climate sensitivity scenarios relative to the baseline scenario. Water and nitrate yields indicate  
 941 the summations of water and nitrate fluxes transported from lands to streams by surface runoff,  
 942 lateral flow, and groundwater flow. PCP and TMP stand for precipitation and temperature,  
 943 respectively. SURQ, LATQ, and GWQ indicate water fluxes transported by surface runoff,  
 944 lateral flow, and groundwater flow, respectively. NSURQ, NLATQ, and NGWQ indicate nitrate  
 945 fluxes transported by surface runoff, lateral flow, and groundwater flow, respectively.

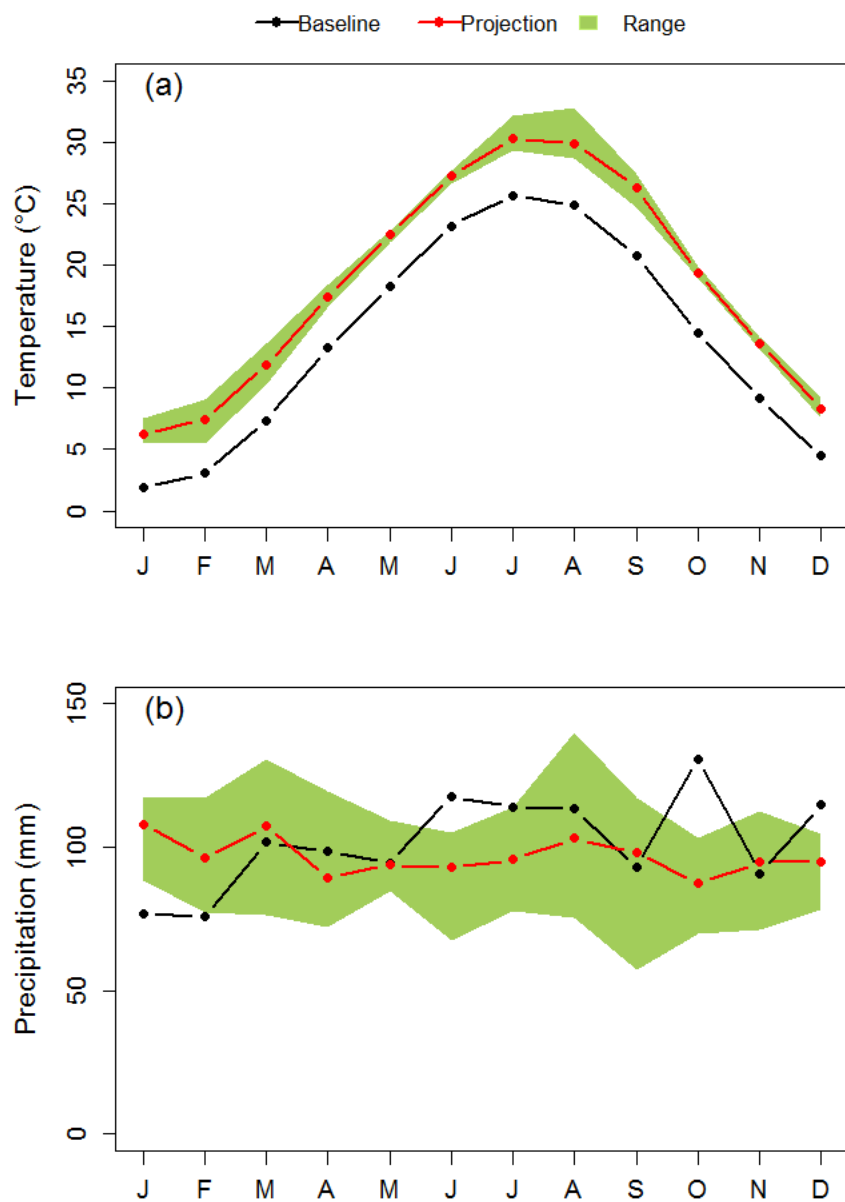
946

947

948

949

950

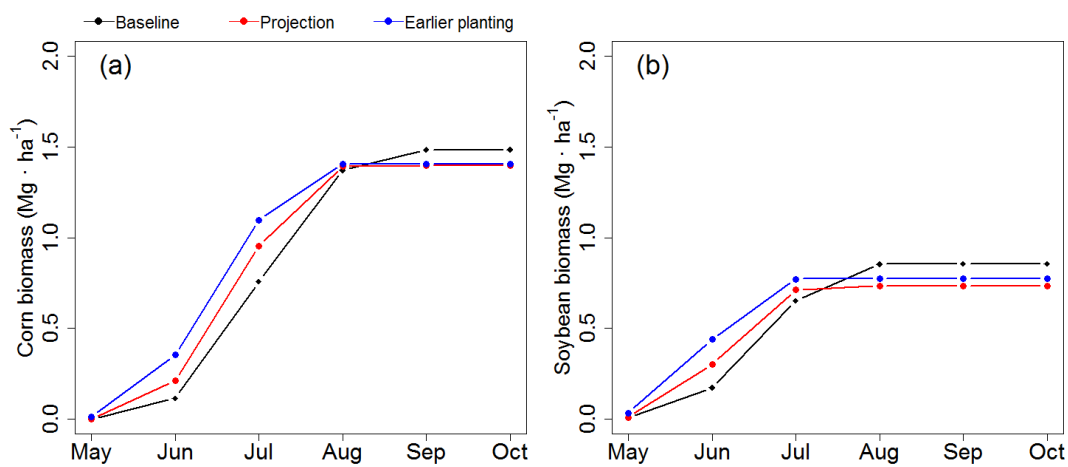


951

952 **Figure 7.** Monthly average of (a) mean temperature and (b) cumulative precipitation for the  
953 baseline (2001 – 2014) and future (2083 – 2098) periods.

954 Note: Projection stands for the ensemble mean of five GCM data, and the range stands for the  
955 interval between the maximum and minimum values of five GCM data.

956



957

958 **Figure 8.** Crop biomass growth under the baseline and climate change scenarios: (a) corn and (b)  
959 soybean.

960 Note: Projection stands for the ensemble mean of simulated biomass with 5 GCMs. Earlier  
961 planting indicates the ensemble mean of simulated biomass planted 10 days earlier than the  
962 original planting dates.

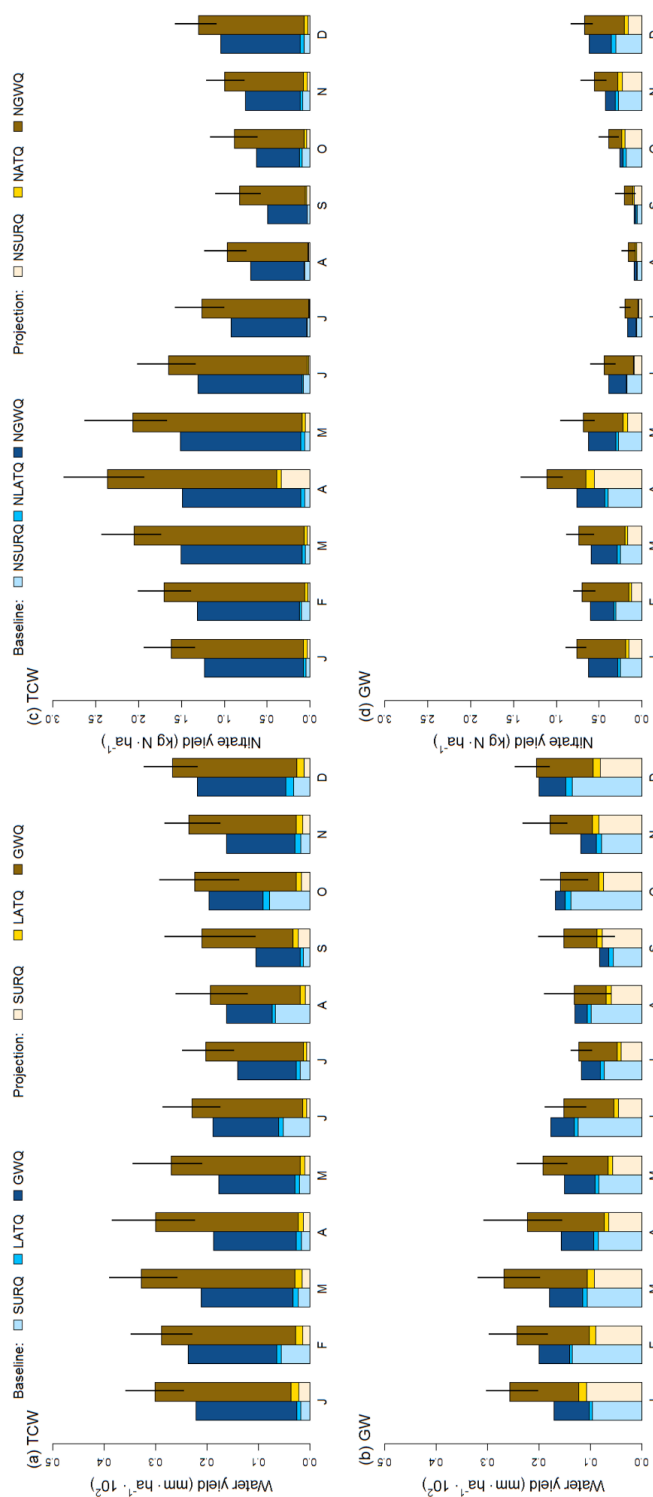


**Figure 9.** 14-year average of monthly water and nitrate yields under the baseline and climate change scenarios.

Note: The descriptions of abbreviation are available in the caption of Figure 6. The black line indicates the interval between minimum and maximum values (water or nitrate yields) of simulation with 5 GCMs.

963

964

965

966

967

968

969



970 **List of Appendices**

971 **Table A1.** Management schedules for the baseline scenario

972 **Table A2.** Five GCMs used to the climate change scenario

973 **Figure A3.** 14-year average of annual mineralized nitrate under the baseline and climate  
974 sensitivity scenarios at the watershed scale.

975 **Figure A4.** Changes in (a & b) soil water content and (c & d) nitrate leaching under temperature  
976 increase

977

978

979

980

981

982

983

984

985

986

987

988



989 **Table A1.** Management schedules for the baseline scenario (adapted from Lee et al. (2016))

Baseline scenario (no winter cover crop)			
Crop	Planting	Fertilizer	Harvest
Corn (after corn)	Apr. 30 (no-till)	157 kg N·ha <sup>-1</sup> (140 lb N·acre <sup>-1</sup> ) of poultry manure on Apr. 20 45 kg N·ha <sup>-1</sup> (40 lb N·ha <sup>-1</sup> ) of sidedress 30% UAN on Jun. 7	Oct. 3
Corn (after Soybean and Double crop soybean)	Apr. 30 (no-till)	124 kg N·ha <sup>-1</sup> (110 lb N·acre <sup>-1</sup> ) of poultry manure on Apr. 20 34 kg N·ha <sup>-1</sup> (30 lb N·ha <sup>-1</sup> ) of sidedress 30% UAN on Jun. 7	Oct. 3
Soybean	May 20 (no-till)		Oct. 15
Double crop winter wheat (Dbl WW)	Oct. 10	34 kg N·ha <sup>-1</sup> (30 lb N·acre <sup>-1</sup> ) of sidedress 30% UAN on Oct. 8 45 kg N·ha <sup>-1</sup> (40 lb N·acre <sup>-1</sup> ) of sidedress 30% UAN on Mar. 1 67 kg N·ha <sup>-1</sup> (60 lb N·acre <sup>-1</sup> ) of sidedress 30% UAN on Apr. 5	Jun. 27
Double crop soybean (Dbl Soyb)	Jun. 29		Nov. 1

990 Note: UAN stands for Urea-Ammonium Nitrate. The typical nitrogen content for poultry manure  
 991 is assumed as 2.8% (Glancey et al., 2012).

992

993

994 **Table A2.** Five GCMs used to the climate change scenario

Num.	Model	Full name	Abbreviation	Agency
1	CCCMA CGCM3.1.1	Canadian Centre for Climate Modelling and Analysis Coupled GCM 3.1.1	CCCMA	Canadian Centre for Climate Modelling and Analysis, Canada
2	CNRM CM3.1	Centre National de Recherches Météorologiques Coupled Global Climate Model, version 3.1	CNRM	National Center of Meteorological Research, France
3	GFDL CM2.0.1	Geophysical Fluid Dynamics Laboratory Climate Model, version 2.0.1	GFDL	Geophysical Fluid Dynamics Laboratory, United States
4	IPSL CM4.1	L'Institut Pierre-Simon Laplace Coupled Model version 4.1	IPSL	L'Institut Pierre-Simon Laplace, France
5	MIROC3.2 (medres)	Model for Interdisciplinary Research on Climate	MIROC	Marine-Earth Science and Technology, Japan

995

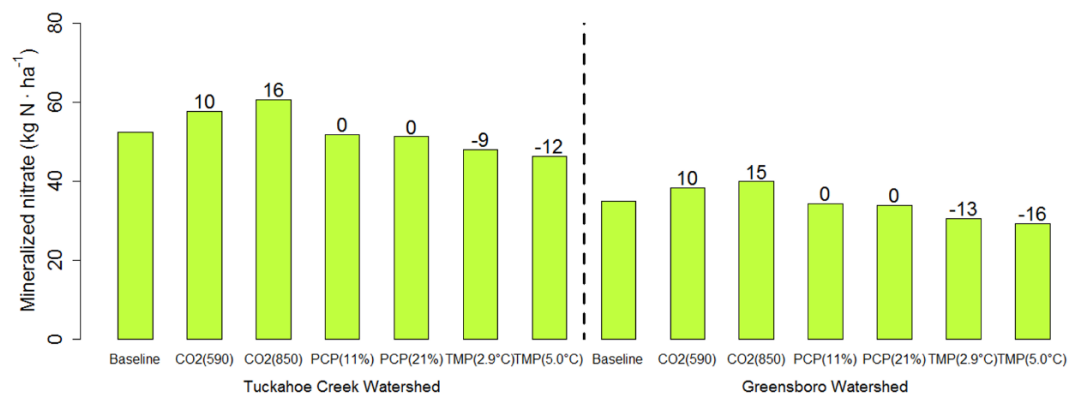
996

997

998

999

1000



1001

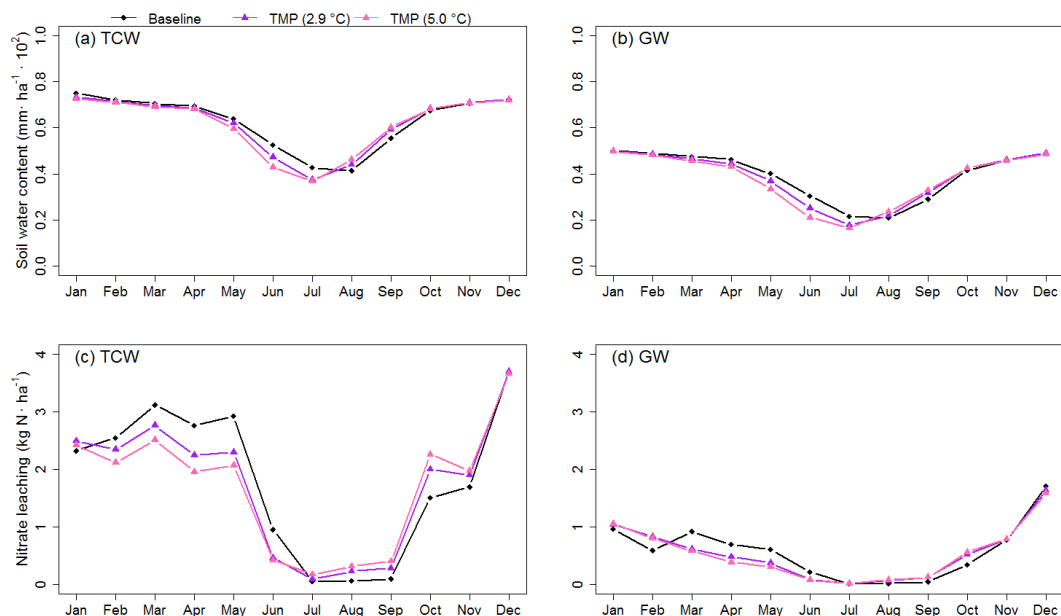
1002 **Figure A3.** 14-year average of annual mineralized nitrate under the baseline and climate  
 1003 sensitivity scenarios at the watershed scale.

1004 Note: The black numerical values above the bar graph indicate the relative changes (%) in  
 1005 hydrologic variables for climate sensitivity scenarios relative to the baseline scenario [relative  
 1006 change (%) = (Sensitivity Scenarios – Baseline) / Baseline × 100]. PCP and TMP stand for  
 1007 precipitation and temperature, respectively.

1008

1009

1010



1011

1012 **Figure A4.** Changes in (a & b) soil water content and (c & d) nitrate leaching under temperature  
 1013 increase

1014 Note: TMP stands for temperature, respectively.